CHAPTER 6
DRAG COEFFICIENTS

Usually, drag experiment will be conducted using smooth sphere and smooth cylinder.

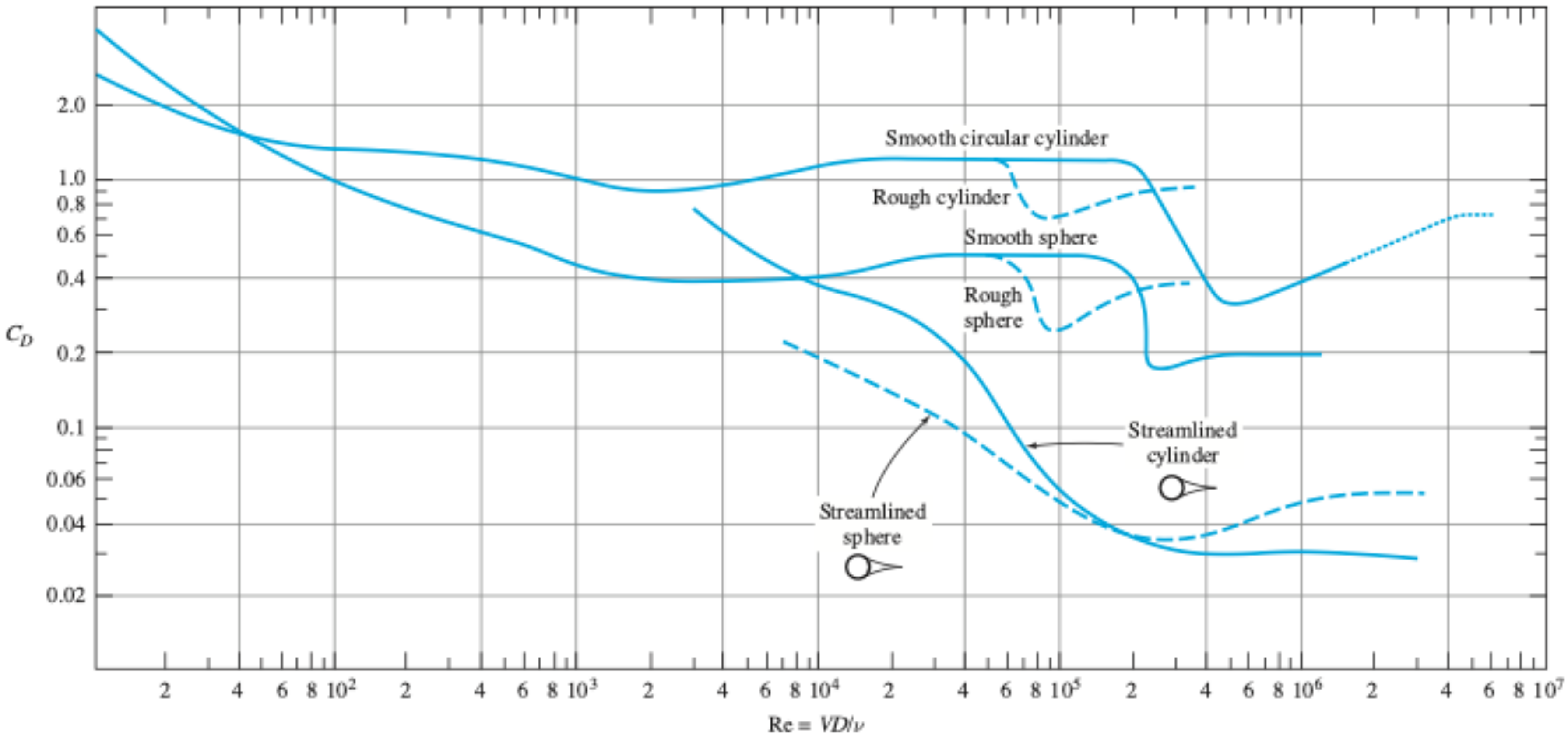

Drag coefficients for flow around a long cylinder and a sphere. (See E. Achenbach, *J. Fluid Mech.*, Vol. 46, 1971, and Vol. 54, 1972.)

(a)

(b)

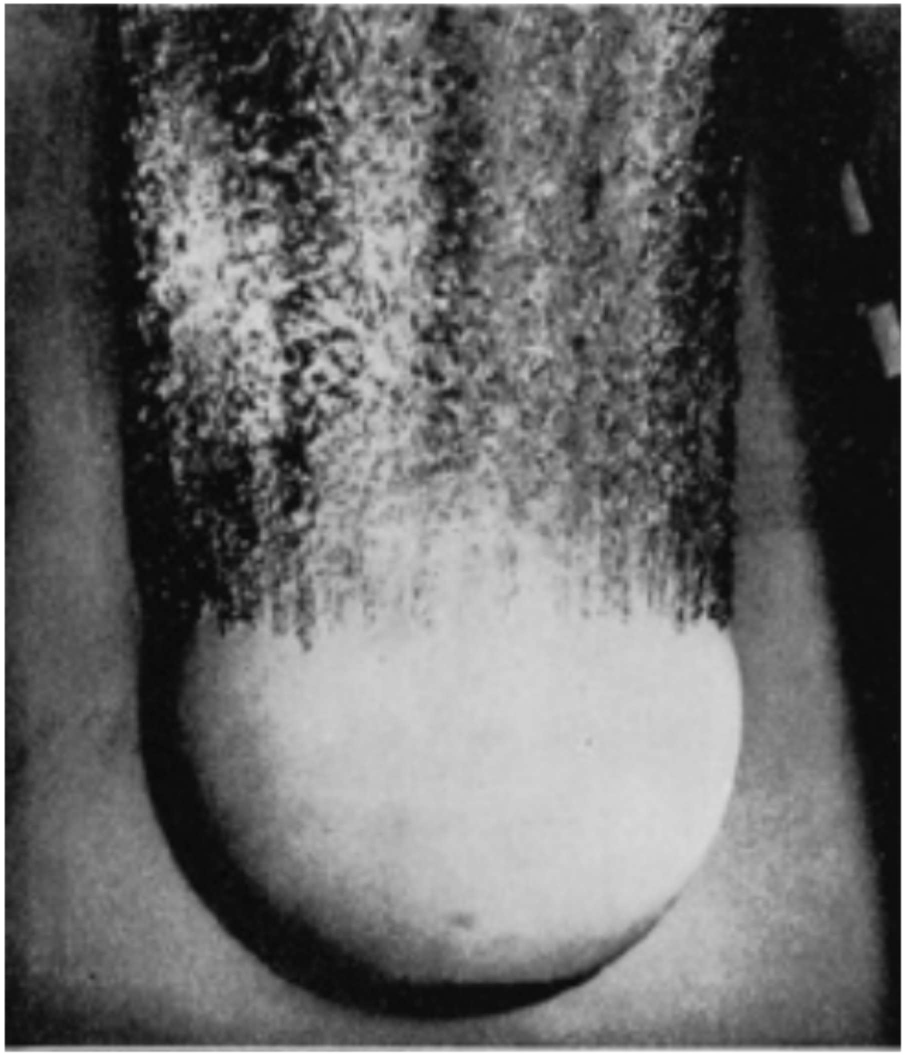

Effect of boundary layer transition on separation:

(a) laminar boundary layer before separation; (b) turbulent boundary layer before separation.

If the experimental works conducted at low Reynolds number, which is Re $<$ 1, it is called a creeping flow.

The value of Reynolds number can be determined as :

$$C_D = \frac{24}{Re} \qquad\qquad Re < 1$$

For creeping flow, separation will not occur.

Separation is observed at $Re \approx 10$ over a very small area on the rear of the body. The separated area increases as the Reynolds number increases until $Re \approx 1000$, where the separated region ceases to enlarge, during this growth of the separated region the drag coefficient decreases.

At $Re \approx 1000$, 95% of the drag is due to form drag (the drag force due to the pressure acting on the body), and 5% is due to frictional drag (the drag force due to the shear stresses acting on the body).

When the boundary layer enters the transition region, the value of drag coefficient is decreased for a while. A rough surface will have transition region earlier compare to those with a smooth surface.

The dimples on the golf ball may increase the flight distance by 50% to 100%.

VORTEX SHEDDING

Long blunt objects, such as circular cylinders, exhibit a particularly interesting phenomenon when placed normal to a fluid flow; vortices or eddies (regions of circulating fluid) are shed from the object, regularly and alternately from opposite sides, as shown below.

The resulting flow downstream is often referred to as a Kármán vortex street, named after Theodor von Kármán (1881–1963). The vortices are shed in the Reynolds number range $40 < \mathrm{Re} < 10\,000$, and are accompanied by turbulence above $\mathrm{Re} = 300$.

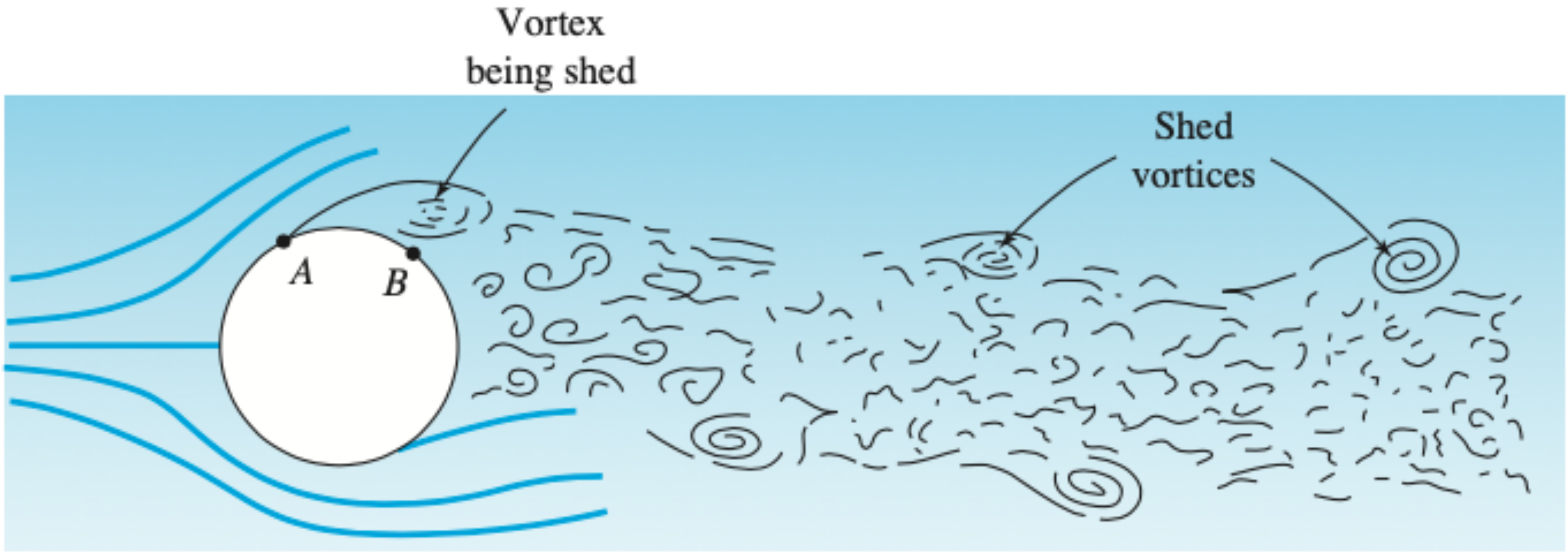

Photographs of high- and low- Reynolds-number vortex shedding are shown below.

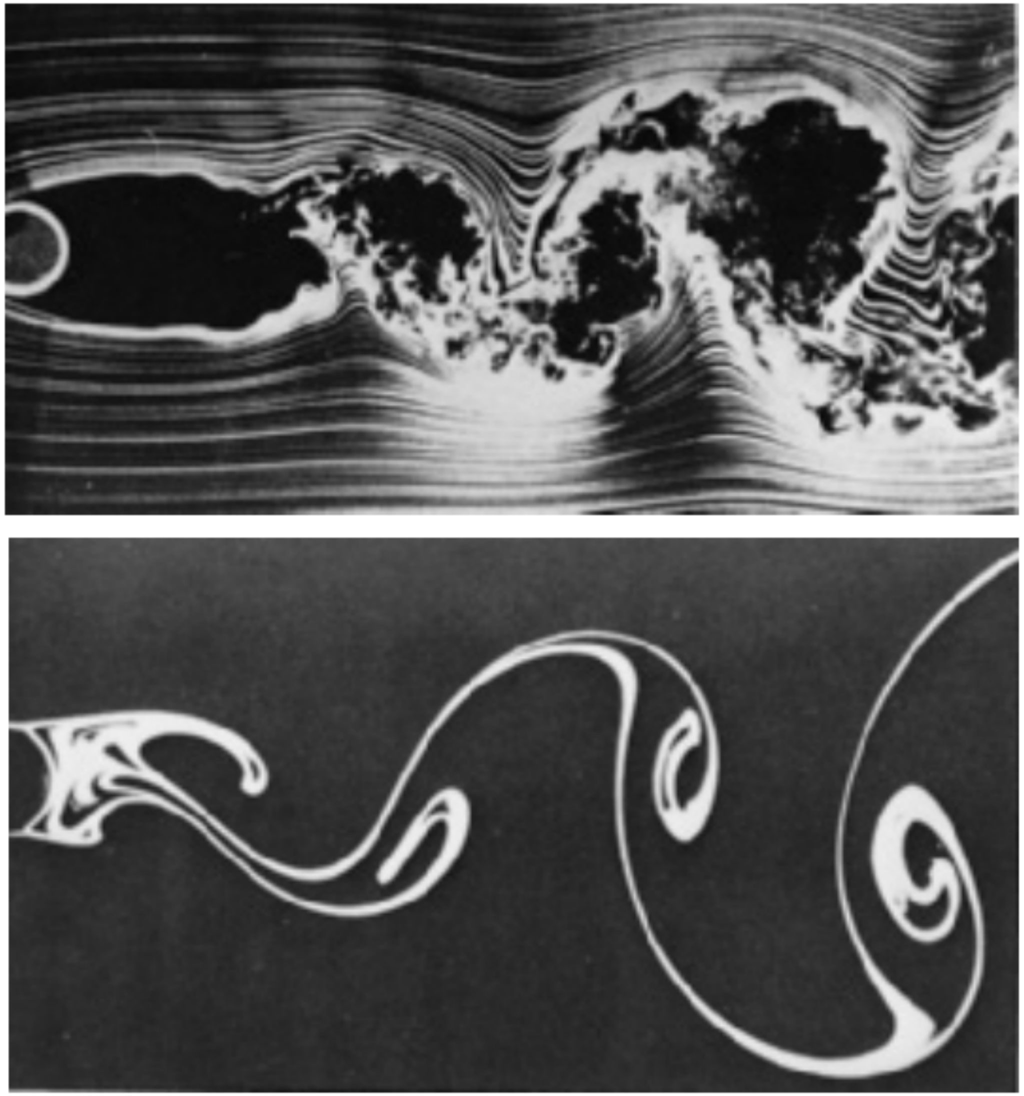

(a)

(b)

Vortex shedding at high and low Reynolds numbers: (a) Re = 10 000 (Photograph by Thomas Corke and Hassan Nagib.); (b) Re = 140 (Photograph by Sadatoshi Taneda. From Album of Fluid Motion, 1982, The Parabolic Press, Stanford, California.)

Dimensional analysis may be applied to find an expression for the shedding frequency.

For high-Reynolds-number flows, that is, flows with insignificant viscous forces, the shedding frequency f, in hertz, depends only on the velocity V and diameter D.

The shedding frequency, expressed as a dimensionless quantity, is expressed as the Strouhal number.

$$St = \frac{fD}{V}$$

From the experimental results as shown below, it is observed that the Strouhal number is essentially constant (0.21) over the range 300 < Re < 10 000; hence, the frequency is directly proportional to the velocity over this relatively large Reynolds number range.

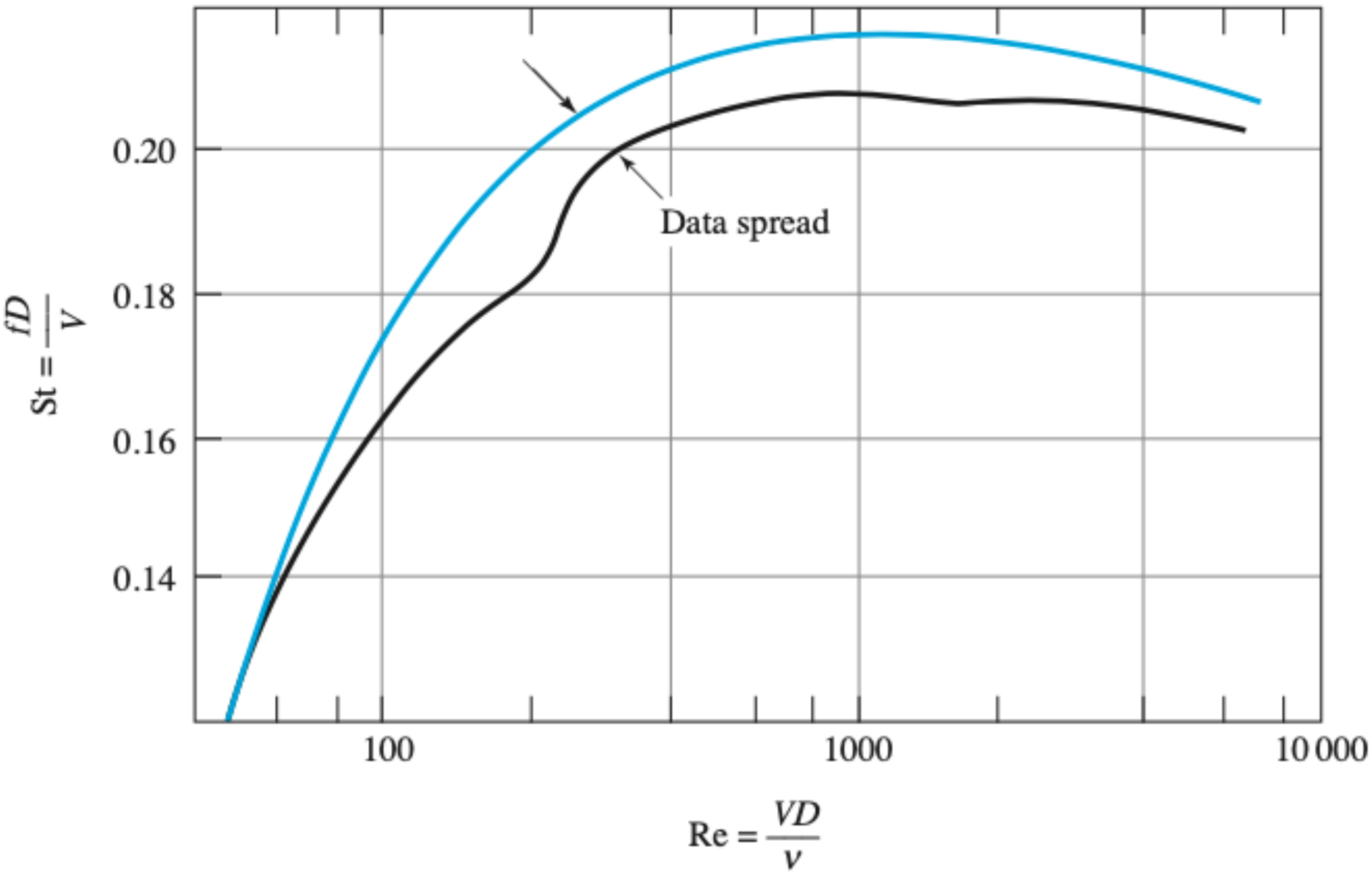

The engineer or architect must be very careful when designing structures, such as towers and bridges, that shed vortices. When a vortex is shed, a small force is applied to the structure; if the frequency of shedding is close to the natural frequency (or one of the harmonics) of the structure, the phenomenon of resonance may occur in which the response to the applied force is multiplied by a large factor.

For example, when resonance occurs on a television tower, the deflection of the tower due to the applied force may become so large that the supporting cables fail, leading to collapse of the structure.

This has occurred many times, leading to severe damage and numerous deaths and injuries. The collapse of the Tacoma Narrows suspension bridge is undoubtedly the most spectacular failure due to vortex shedding.

"Galloping" power lines, in which a power line alternates between the usual catenary and an inverted catenary, is another example that may lead to significant damage; this may occur when a power line has iced up, providing a much larger cross-sectional area for the wind.

Tacoma Narrow Bridge

Galloping wire

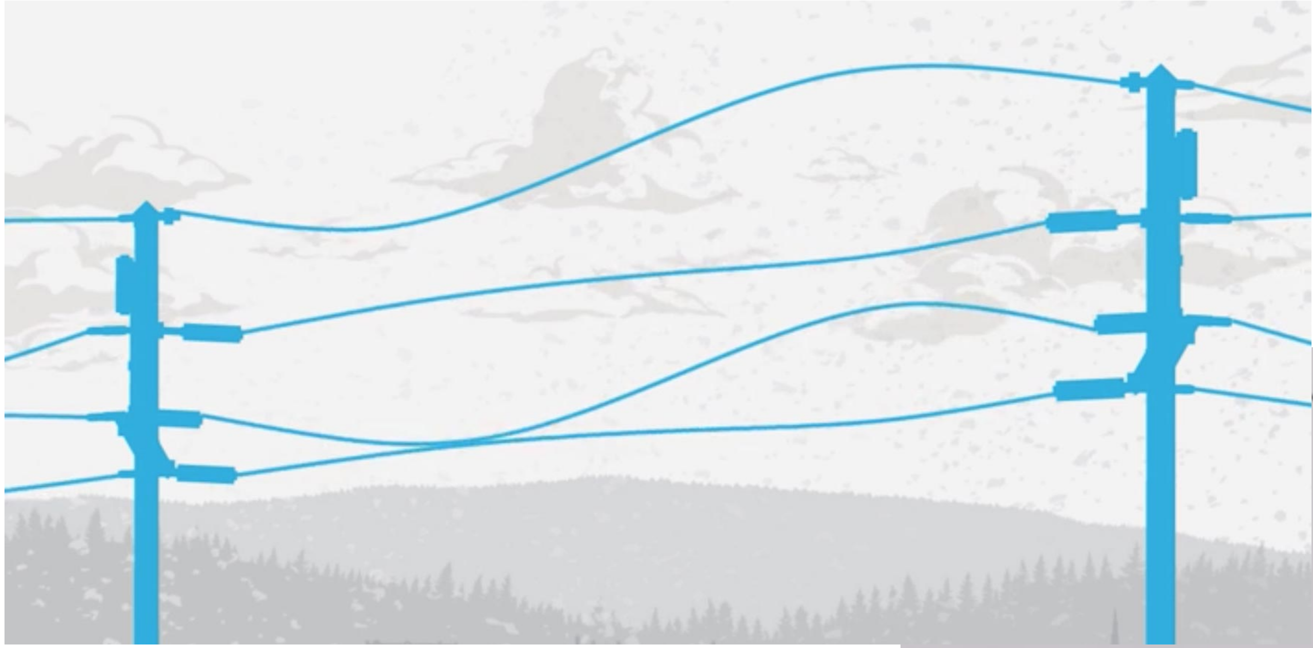

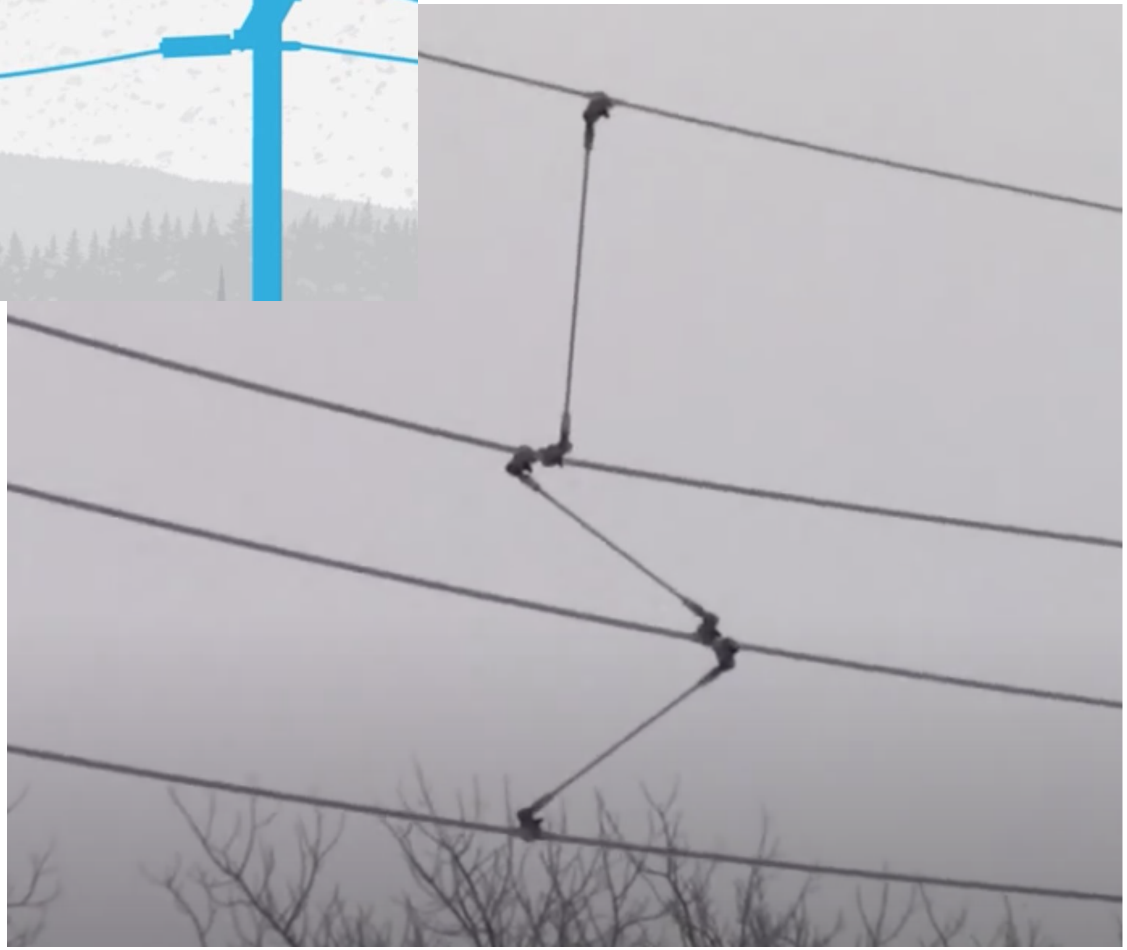

STREAMLINING

If the flow is to remain attached to the surface of a blunt object, such as a cylinder or a sphere, it must move into regions of higher and higher pressure as it progresses to the rear stagnation point.

At sufficiently high Reynolds numbers ($Re > 10$) the slow-moving boundary layer flow near the surface is unable to make its way into the high-pressure region near the rear stagnation point, so it separates from the object.

Streamlining reduces the high pressure at the rear of the object so that the slow-moving flow near the surface is able to negotiate its way into a slightly higher-pressure region. The fluid may not be able to make it all the way to the trailing edge of the streamlined object, but the separation region will be reduced to only a small percentage of the initial separated region on the blunt object.

The included angle at the trailing edge must not be greater than about 20° or the separation region will be too large, and the effect of streamlining will be negated.

Drag coefficients for streamlined cylinders and spheres are lower compare to the cylinder and sphere without streamlining.

A circular cylinder and a streamlined cylinder

The streamlined cylinder will have lower drag coefficient, and this will lead to the lower drag force.

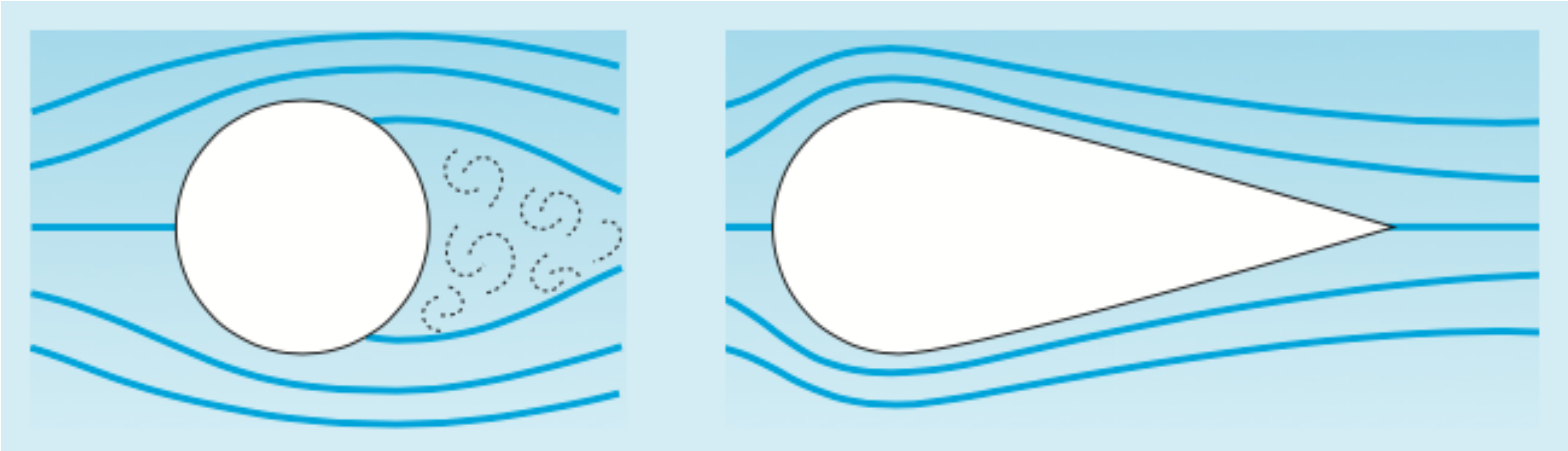

CAVITATION

Cavitation is a very rapid change of phase from liquid to vapor which occurs in a liquid whenever the local pressure is equal to or less than the vapor pressure. The first appearance of cavitation is at the position of lowest pressure in a field of flow. Four types of cavitation have been identified:

1. Traveling cavitation, which exists when vapor bubbles or cavities are formed, are swept downstream, and collapse.

2. Fixed cavitation, which exists when a fixed cavity of vapor exists as a separated region. The separated region may reattach to the body, or the separated region may enclose the rear of the body and be closed by the main flow, in which case it is referred to as supercavitation.

3. Vortex cavitation, which is found in the high-velocity, and thus low-pressure, core of a vortex, often observed in the tip vortex leaving a propeller.

4. Vibratory cavitation, which may exist when a pressure wave moves in a liquid. A pressure wave consists of a pressure pulse, which has a high pressure followed by a low pressure. The low-pressure part of the wave (or vibration) can result in cavitation.

Traveling cavitation

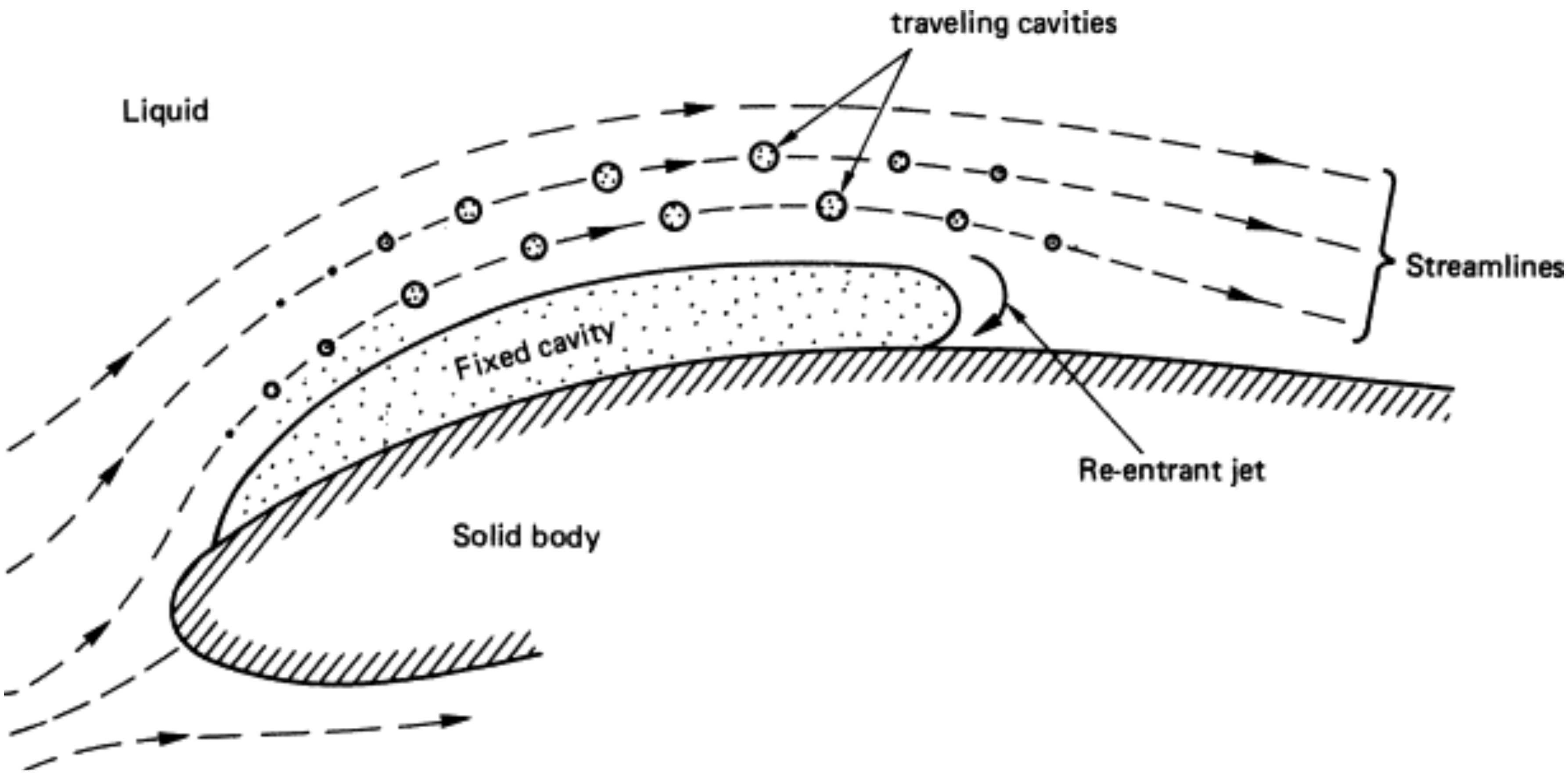

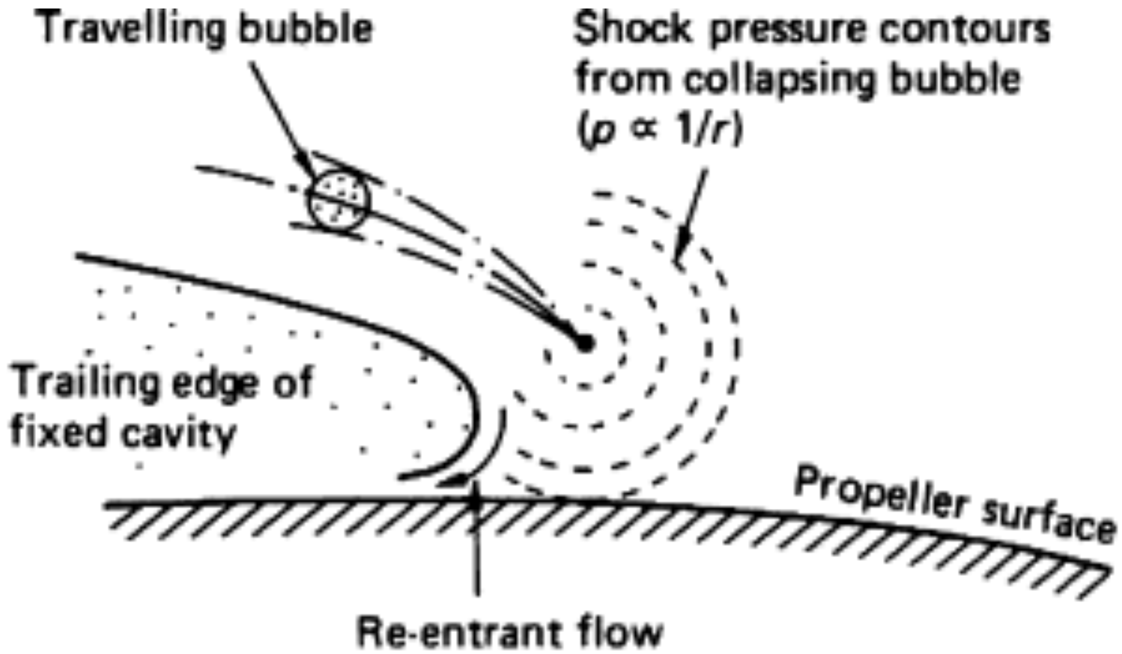
Travelling bubble
Shock pressure contours
from collapsing bubble
($p \propto 1/r$)
Trailing edge of
fixed cavity
Propeller surface
Re-entrant flow

(a)

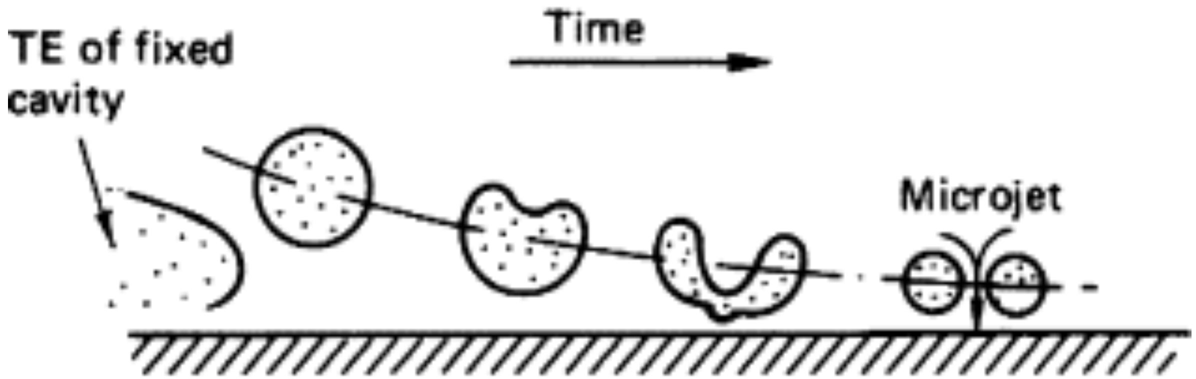
Time
TE of fixed
cavity
Microjet

(b)

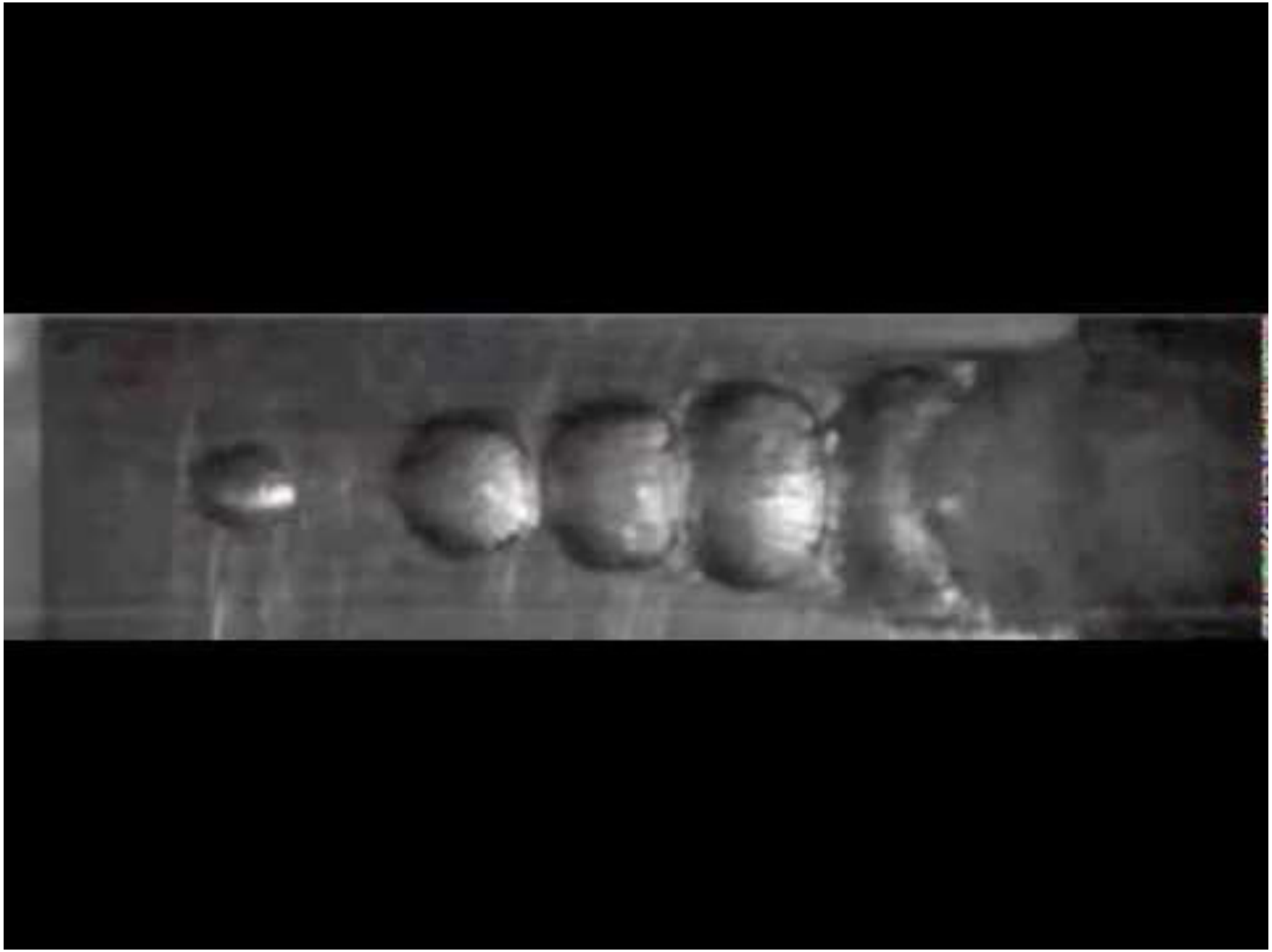

Supercavitation

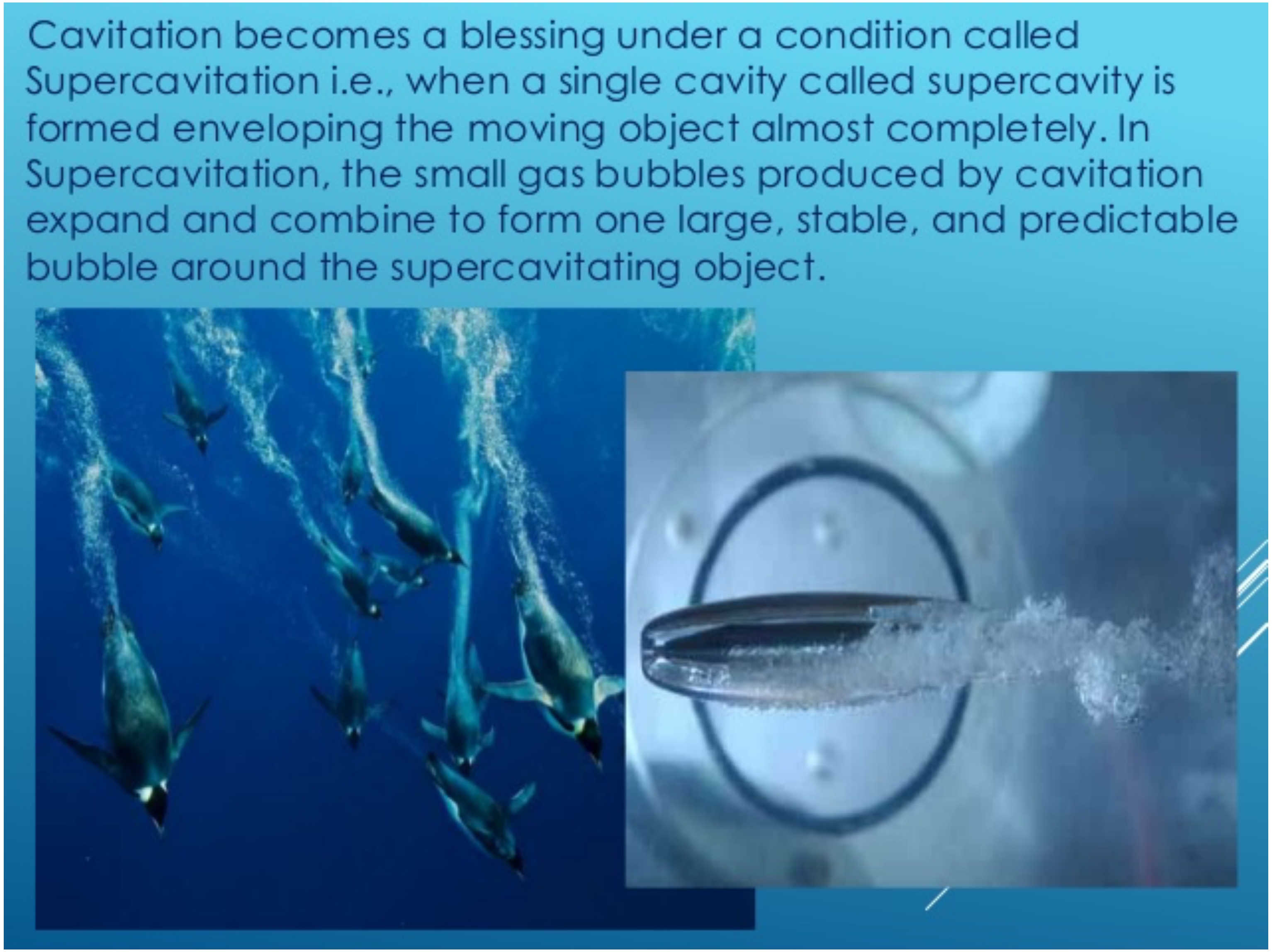

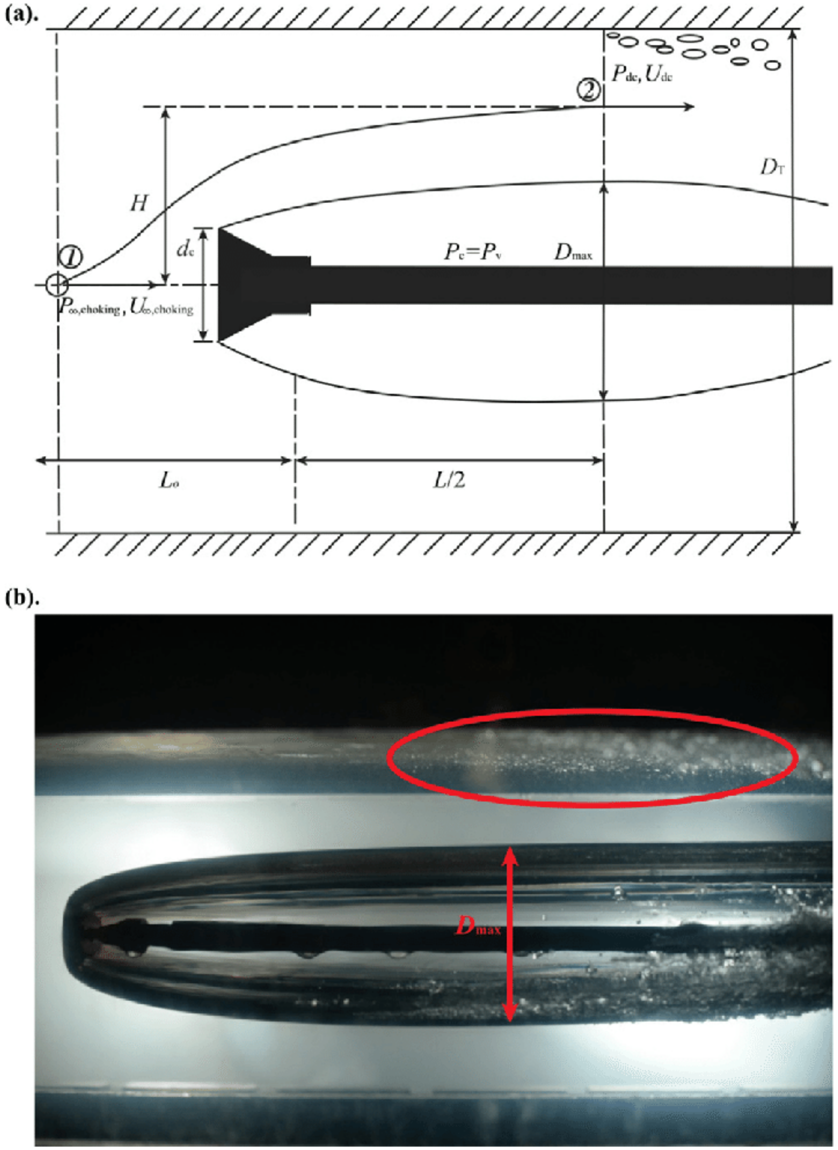
(a).
2
P_dc, U_dc
D_T
H
1
d_c
P_c=P_v
D_max
P_∞,choking, U_∞,choking
L_o
L/2
(b).
D_max

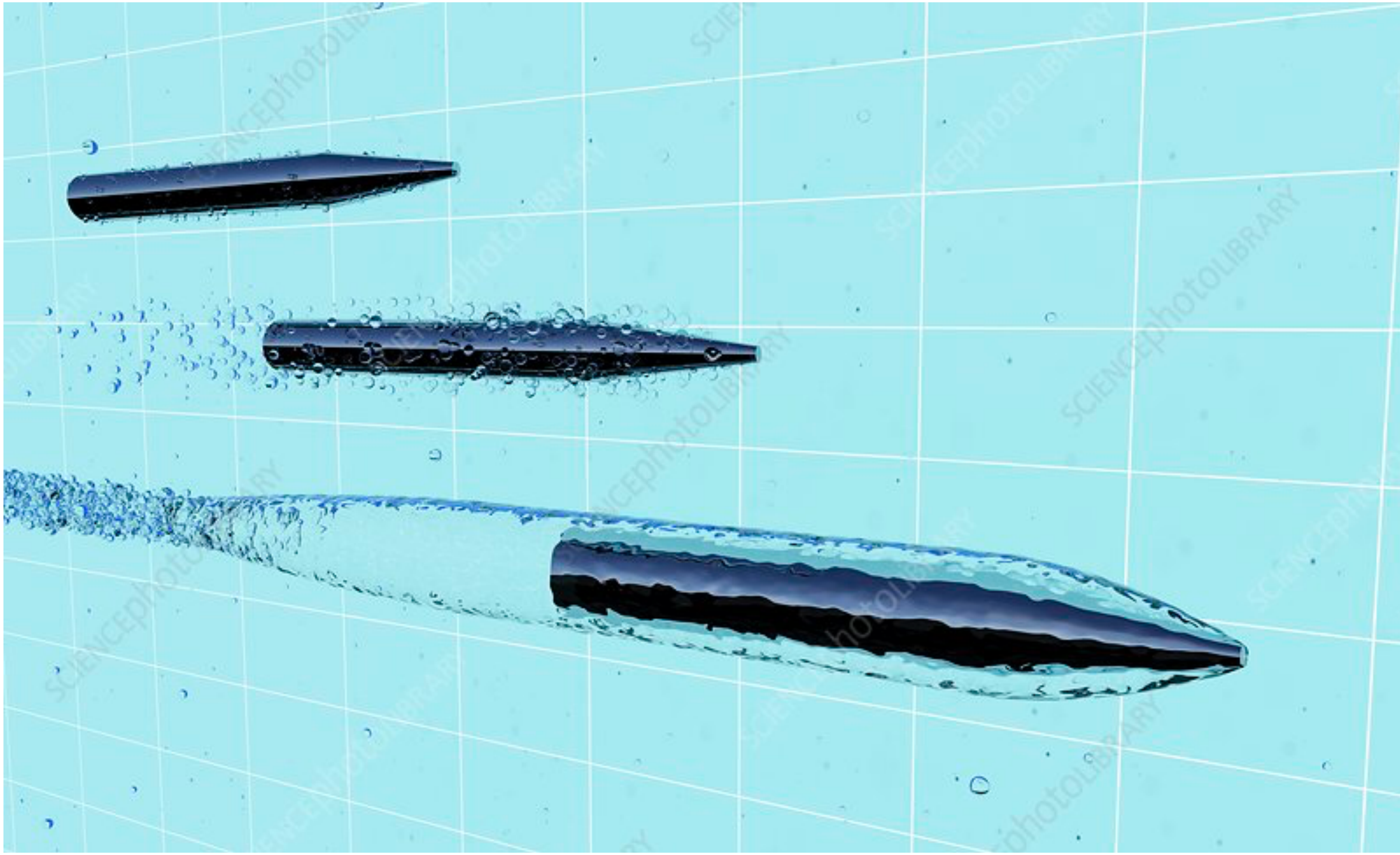

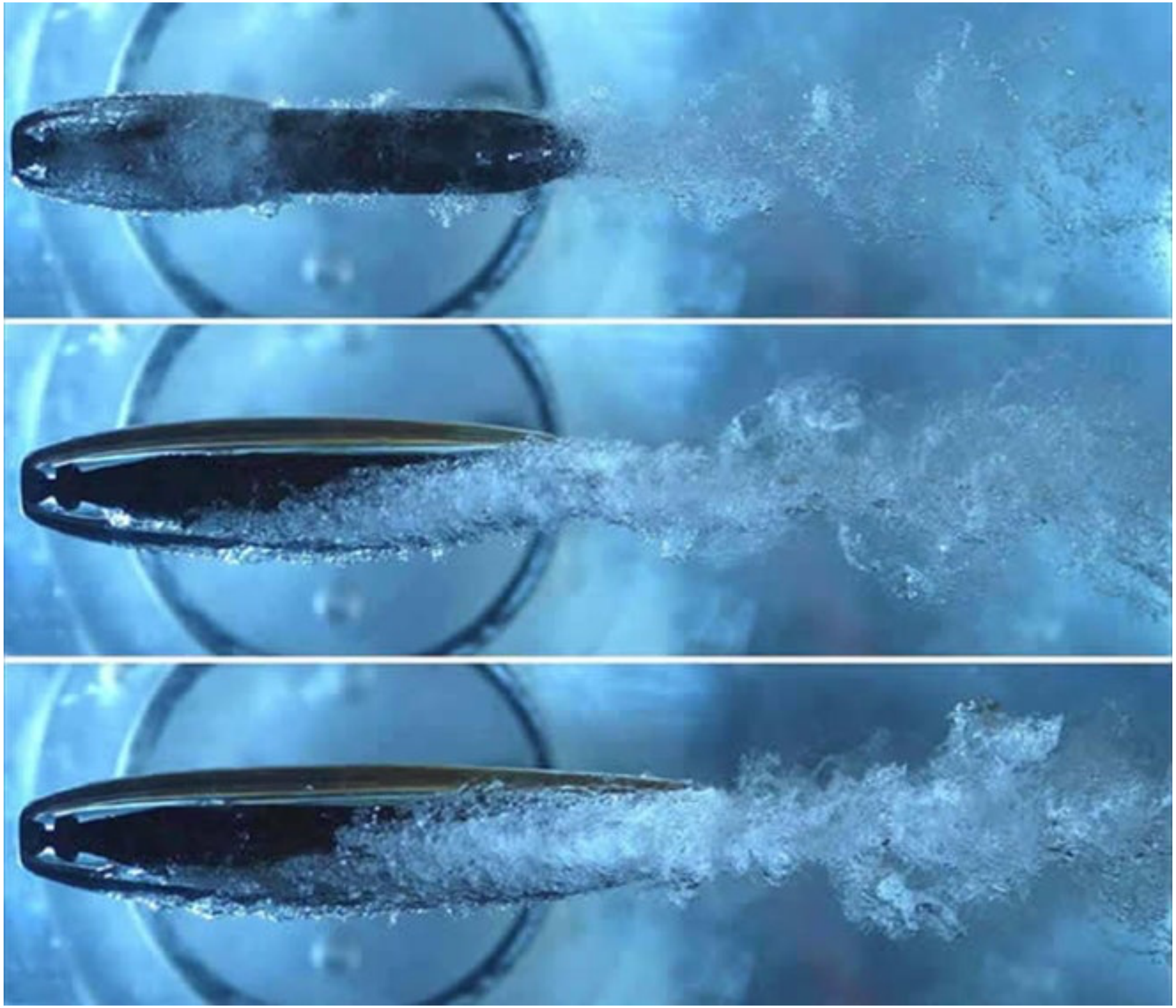

Vortex cavitation

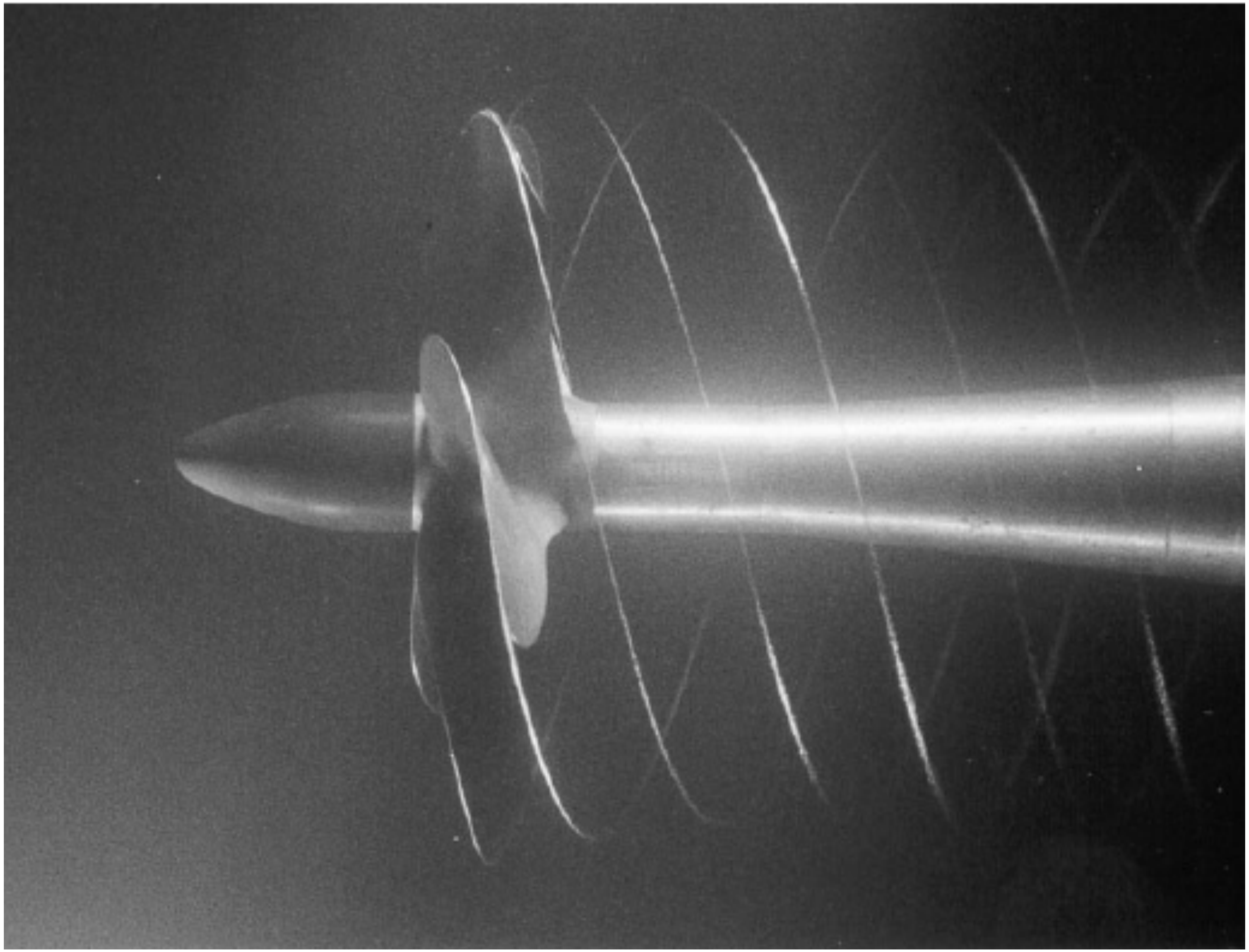

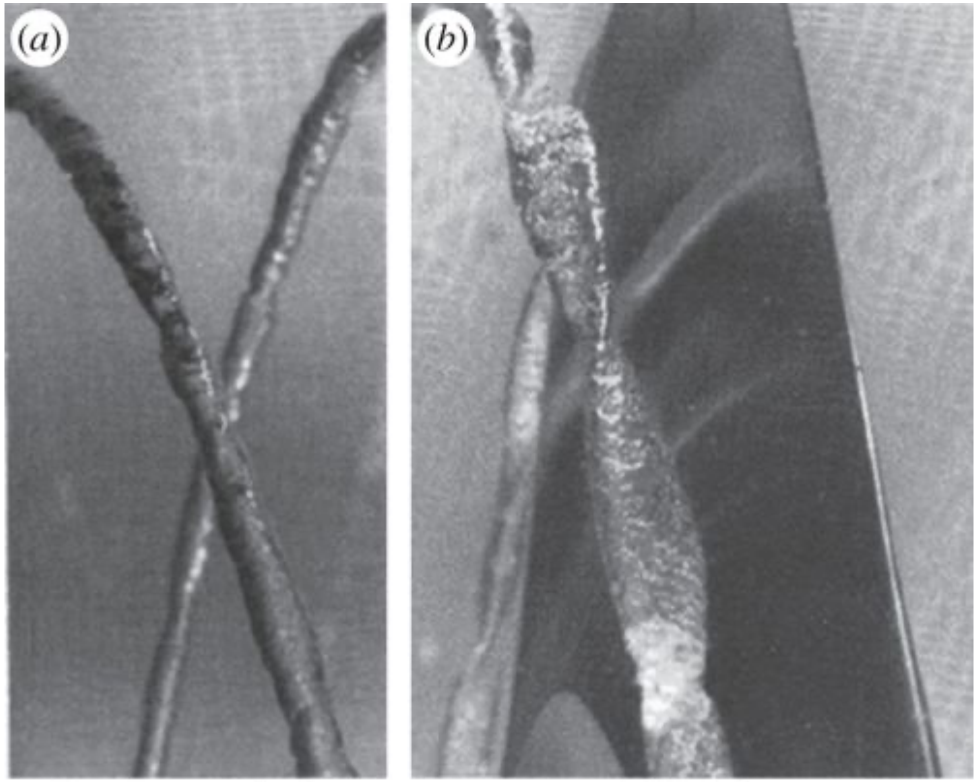

after one revolution   behind tip

Vibratory cavitation

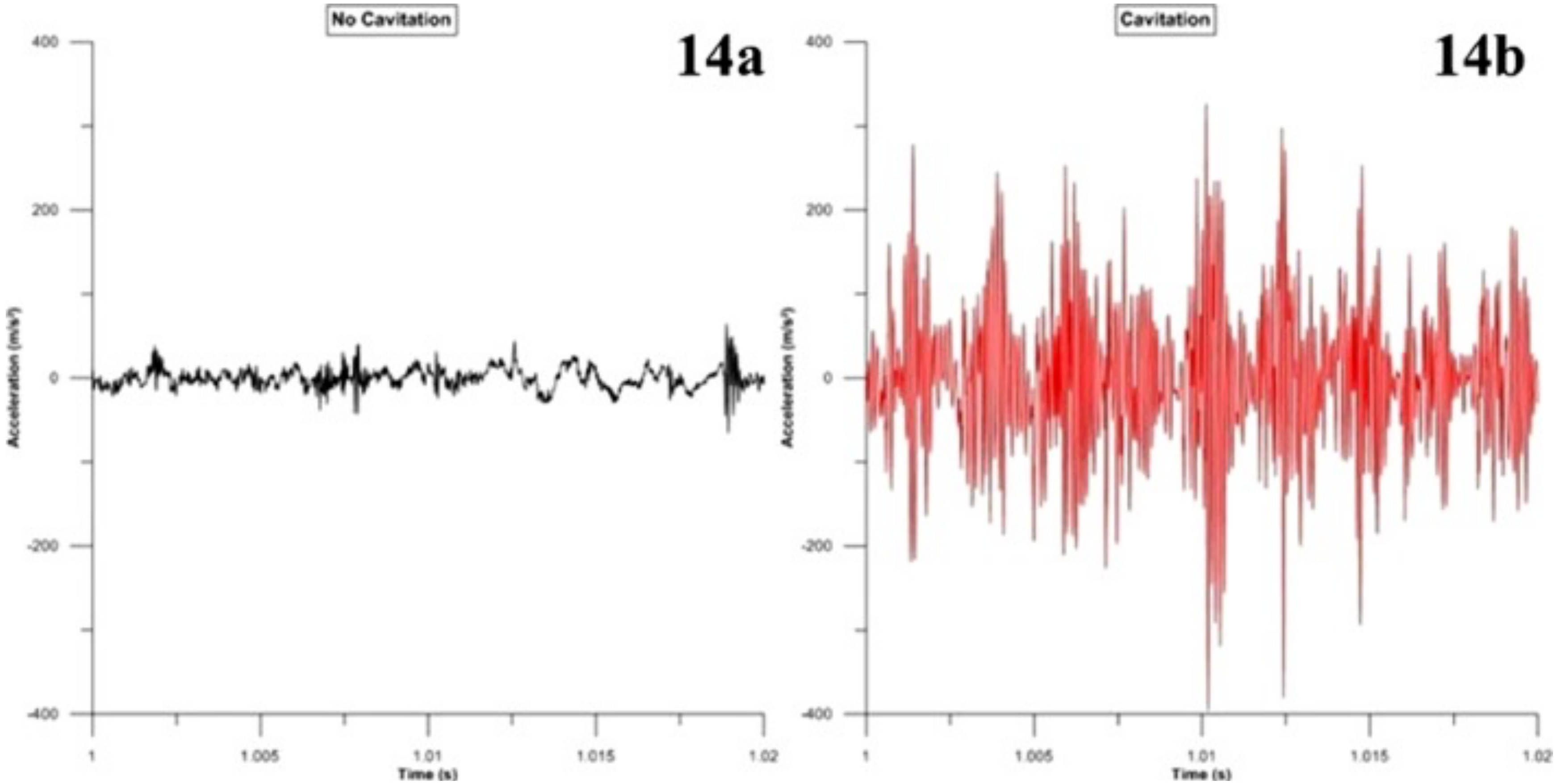

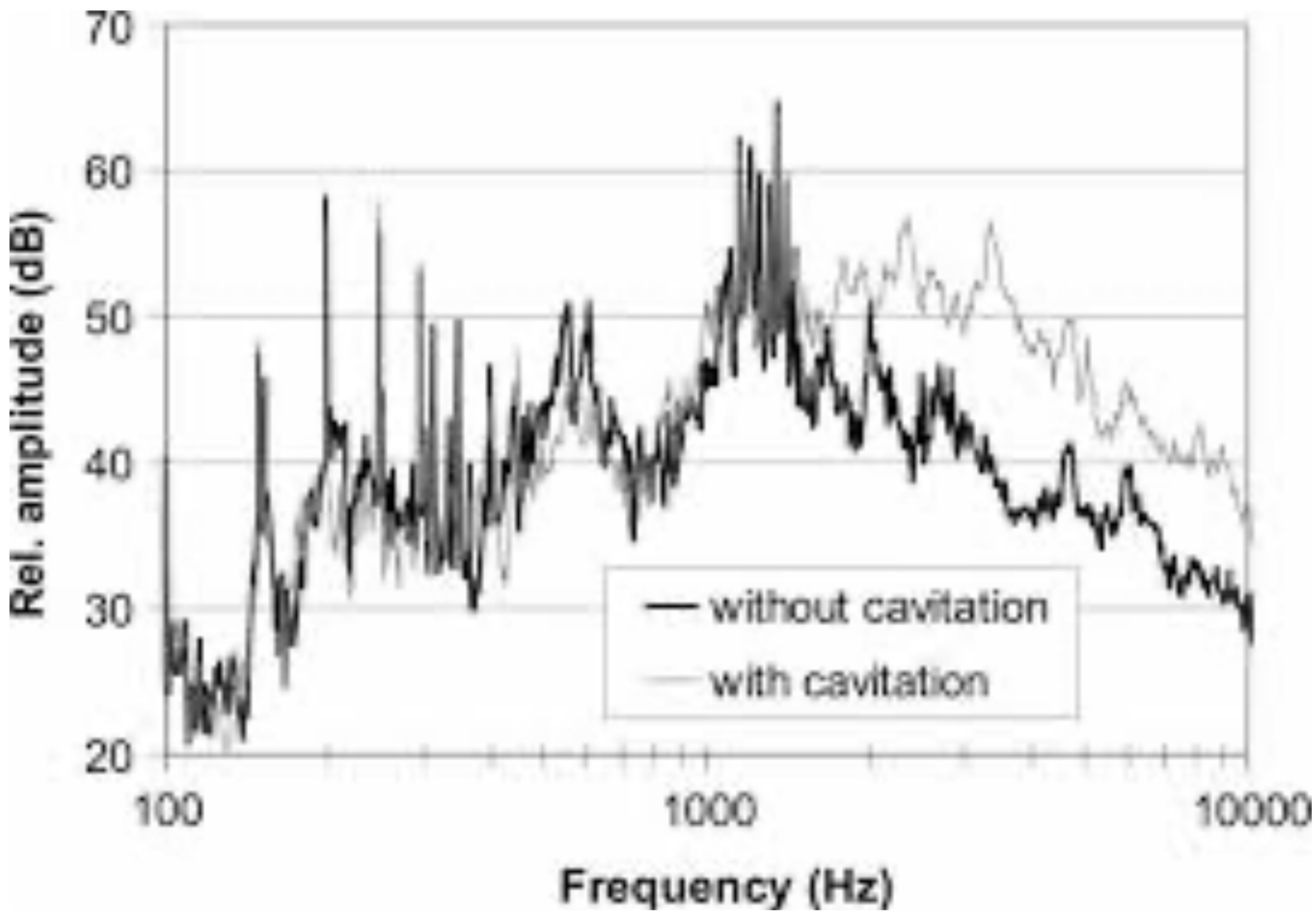
70
60
50
40
30
20
Rel. amplitude (dB)
100
1000
10000
Frequency (Hz)
without cavitation
with cavitation

Cavitation number, σ

The first type of cavitation, in which vapor bubbles are formed and collapse, is associated with potential damage. The instantaneous pressures resulting from the collapse can be extremely high (perhaps 1400 MPa) and may cause damage to stainless steel components, as happens on the propellers of ships.

Cavitation occurs whenever the cavitation number, σ , is less than the critical cavitation number, $\sigma_{critical}$, which depends on the geometry of the body and the Reynolds number. Here p_∞ is the absolute pressure in the undisturbed free stream and p_v is the vapor pressure. As σ decreases below $\sigma_{critical}$, the cavitation increases in intensity, moving from traveling cavitation to fixed cavitation to supercavitation.

$$\sigma = \frac{p_\infty - p_v}{\frac{1}{2}\rho V^2}$$

Below here, is a few examples of C_D for common shapes for $Re = 10^5$.

Drag Coefficients for Zero Cavitation Number for Blunt Objects

Two-dimensional body				*Axisymmetric body*		
Geometry		θ	$C_D(0)$	*Geometry*	θ	$C_D(0)$
Flat plate		—	0.88	Disk	—	0.8
Circular cylinder		—	0.50	Sphere	—	0.30
		120	0.74	Cone	120	0.64
Wedge	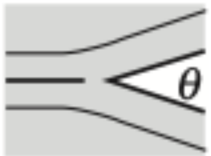	90	0.64	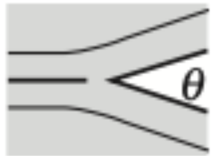	90	0.52
		60	0.49		60	0.38
		30	0.28		30	0.20

The hydrofoil, an airfoil-type body that is used to lift a vessel out of the water, is a shape that is invariably associated with cavitation. Drag and lift coefficients and critical cavitation numbers are shown in the table. For a typical hydrofoil with $10^5 < \mathrm{Re} < 10^6$, where the Reynolds number is based on the chord length and the area used with C_D and C_L is the chord times the length.

Drag and Lift Coefficients and Critical Cavitation Number for a Typical Hydrofoil

Angle (°)	*Lift coefficient* C_L	*Drag coefficient* C_D	*Critical cavitation number* σ_{crit}
−2	0.2	0.014	0.5
0	0.4	0.014	0.6
2	0.6	0.015	0.7
4	0.8	0.018	0.8
6	0.95	0.022	1.2
8	1.10	0.03	1.8
10	1.22	0.04	2.5

LIFT AND DRAG ON AIRFOILS
Separation on an airfoils

Separation occurs on a blunt body, such as a cylinder, due to the strong adverse pressure gradient in the boundary layer on the rear of the body. An airfoil is a streamlined body designed to reduce the adverse pressure gradient so that separation will not occur, usually with a small angle of attack, as shown in the figure below. Without separation the drag is due primarily to the wall shear stress, which results from viscous effects in the boundary layer.

The boundary layer on an airfoil is very thin, and thus it can be ignored when solving for the flow field (the streamline pattern and the pressure distribution) surrounding the airfoil. Since the boundary layer is so thin, the pressure on the wall is not significantly influenced by the boundary layer's existence.

Hence the lift on an airfoil can be approximated by integrating the pressure distribution as given by the inviscid flow solution on the wall. In the next section we will demonstrate how this is done; in this section we simply give empirical results.

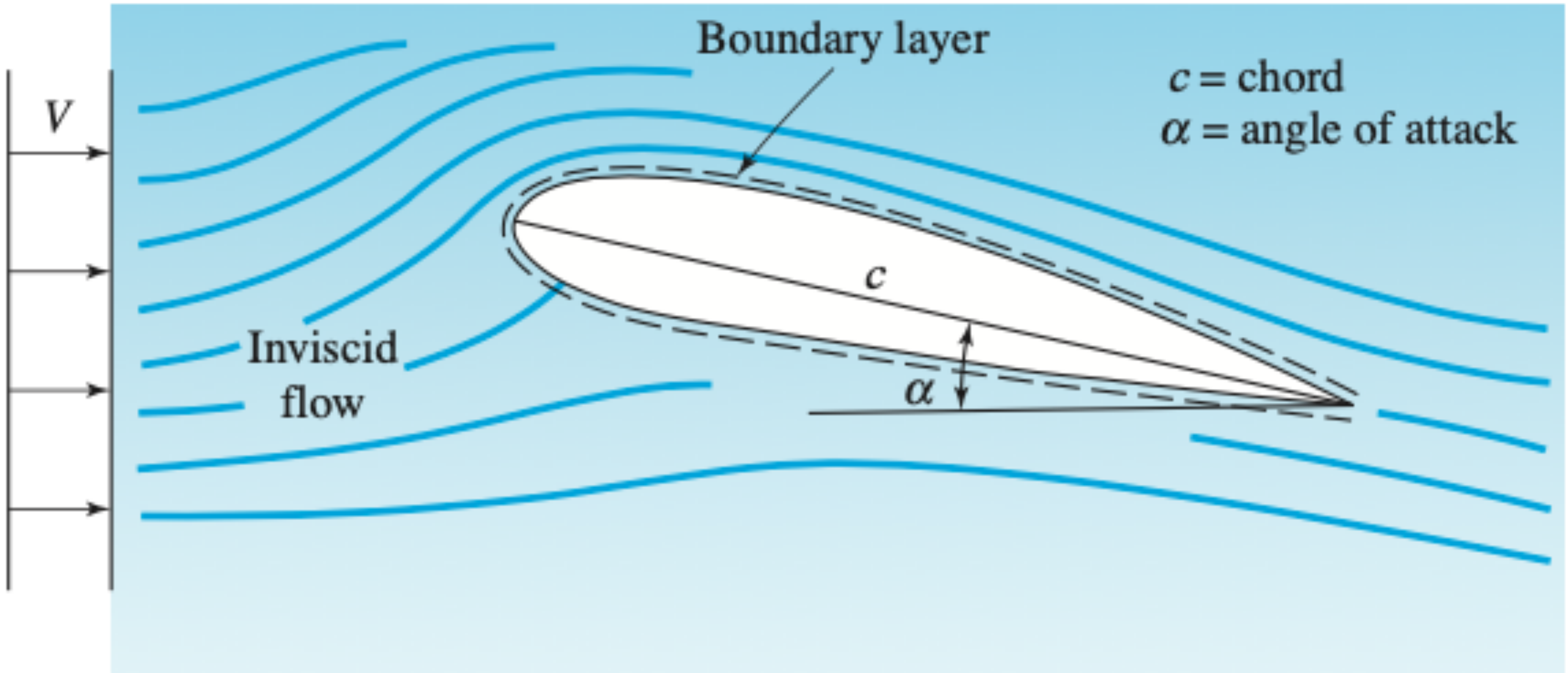

Flow around an airfoil at an angle of attack.

Drag force and lift force

The drag on an airfoil can be predicted by solving the boundary layer equations (simplified Navier–Stokes equations) for the shear stress on the wall and performing the appropriate integration. The inviscid flow field must be known before the boundary layer equations can be solved since the pressure gradient on the wall and the inviscid flow velocity at the wall are needed as inputs in solving for the boundary layer flow.

For airfoils, a much larger projected area is used, namely, the plan area, which is the chord c times the length L of the airfoil. Thus, the drag and lift coefficients are defined as:

$$C_D = \frac{F_D}{\frac{1}{2}\rho V^2 (cL)}$$

$$C_L = \frac{F_L}{\frac{1}{2}\rho V^2 (cL)}$$

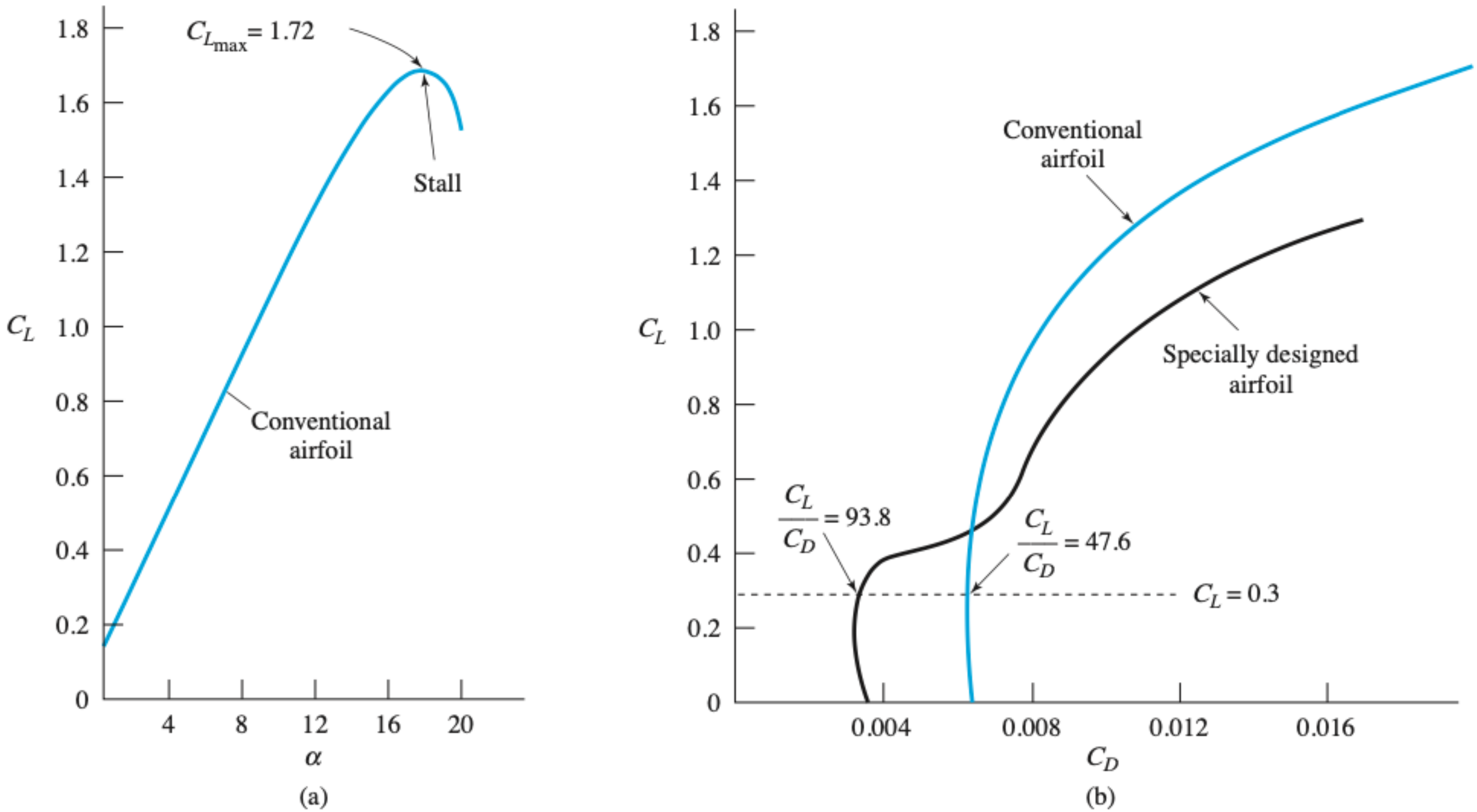

Lift and drag coefficients for airfoils with $\mathrm{Re} = Vc/\nu \simeq 9 \times 10^6$.

For a typical airfoil the lift and drag coefficients are given in figure above.

For a specially designed airfoil the drag coefficient may be as low as 0.0035, but the maximum lift coefficient is about 1.5. The design lift coefficient (cruise condition) is about 0.3, which is near the minimum drag coefficient condition. This corresponds to an angle of attack of about 2°, far from the stall condition of about 16°.

Conventional airfoils are not symmetric; hence there is a positive lift coefficient at zero angle of attack. The lift is directly proportional to the angle of attack but deviates from the straight-line function just before stall.

The drag coefficient also increases linearly up to an angle of attack of about five degrees for a conventional airfoil Then, it increases in a nonlinear relation with angle of attack.

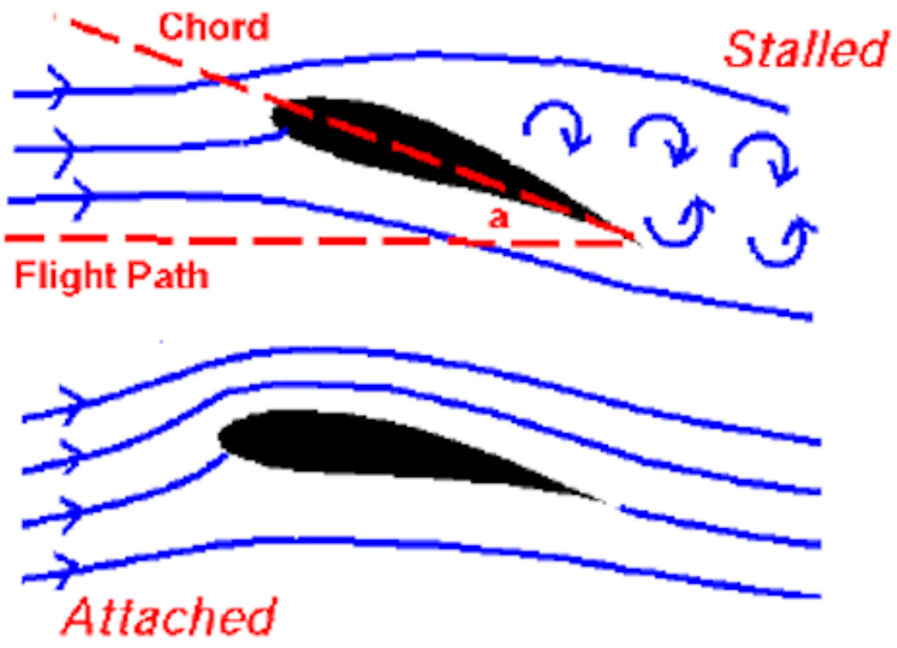

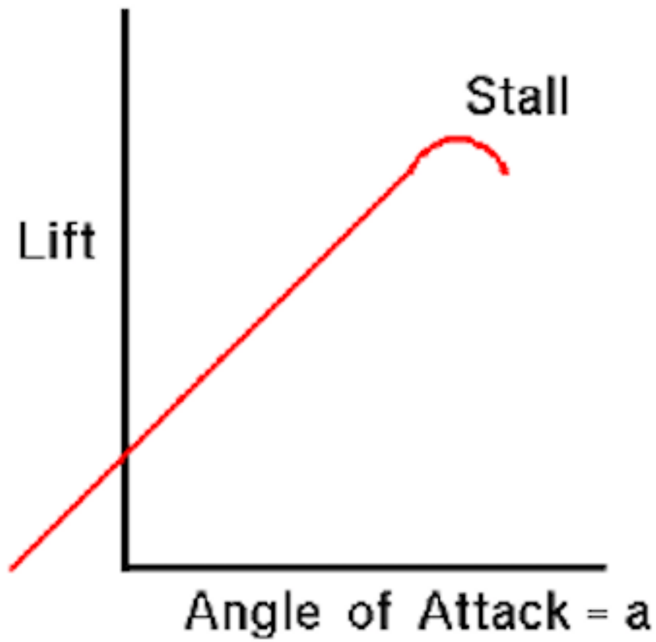

For small angles, lift is related to angle.

Greater Angle = Greater Lift

For larger angles, the lift relation is complex.

Included in Lift Coefficient

Slot and flap on the airfoil

To take off and land at relatively low speeds, it is necessary to attain significantly higher lift coefficients than the maximum of 1.7 (See above figure). Or if a relatively low lift coefficient is to be accepted, the area $c \times L$ must be enlarged. Both are actually accomplished.

Flaps are moved out from a section of each airfoil, resulting in an increased chord, and the angle of attack of the flap is also increased. Slots are used to move high-pressure air from the underside into the relatively low momentum boundary layer flow on the top side, as shown in the figure.

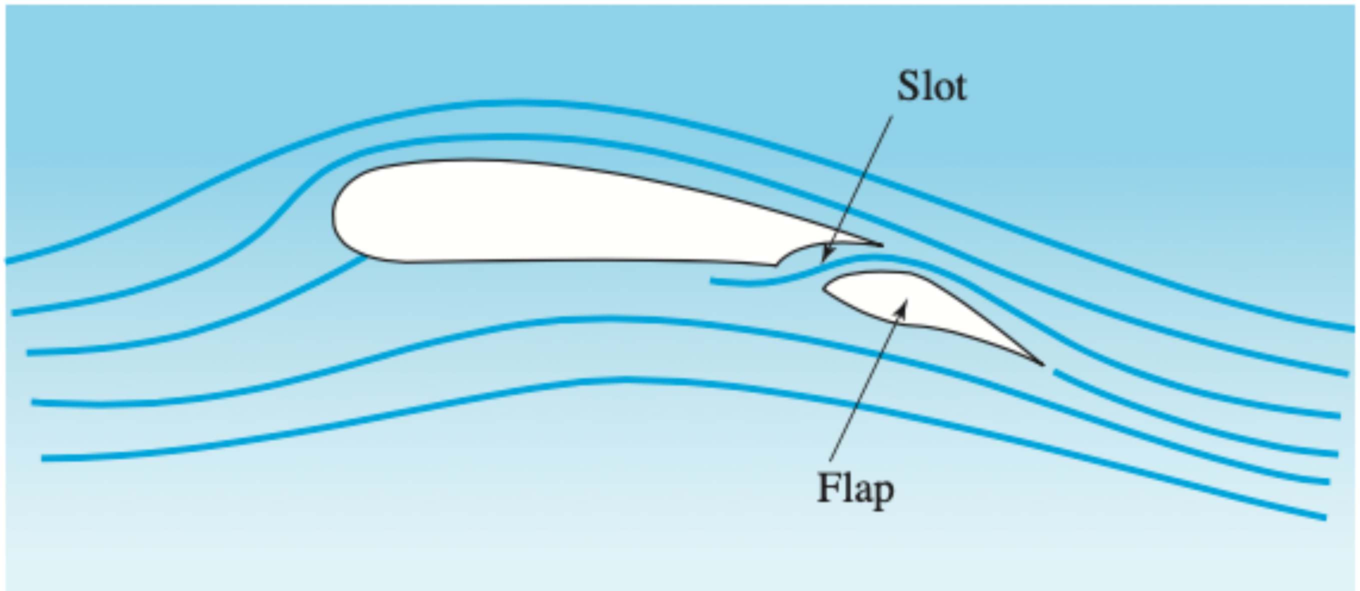

Flapped airfoil with slot for separation control.

This prevents separation from the flap, thereby maintaining high lift.

The lift coefficient can reach 2.5 with a single-slotted flap and 3.2 with a double-slotted flap.

On some modern aircraft there may be three flaps in series with three slots along with a nose flap, to ensure that the boundary layer does not separate from the upper surface of the airfoil.

The total lift on an aircraft is supplied primarily by the airfoil. The effective length of the airfoil when calculating the lift is taken to be the tip-to-tip distance, the wingspan, since the fuselage acts to produce lift on the midsection of the aircraft. The drag calculation must include the shear acting on the airfoil, the fuselage, and the tail section.

The drag coefficient is essentially constant on airfoils up to a Mach number of about 0.75. Then a sudden rise occurs until the Mach number reaches unity ($M = 1$).

The drag coefficient then slowly falls. Obviously, the condition of $M=1$ is to be avoided. Thus, aircraft fly at either $M < 0.75$ or $M > 1.5$ or so, to avoid the high drag coefficients near $M = 1$.

Near $M = 1$, there are also regions of flow that oscillate from subsonic to supersonic. Such oscillations create forces that are best avoided.

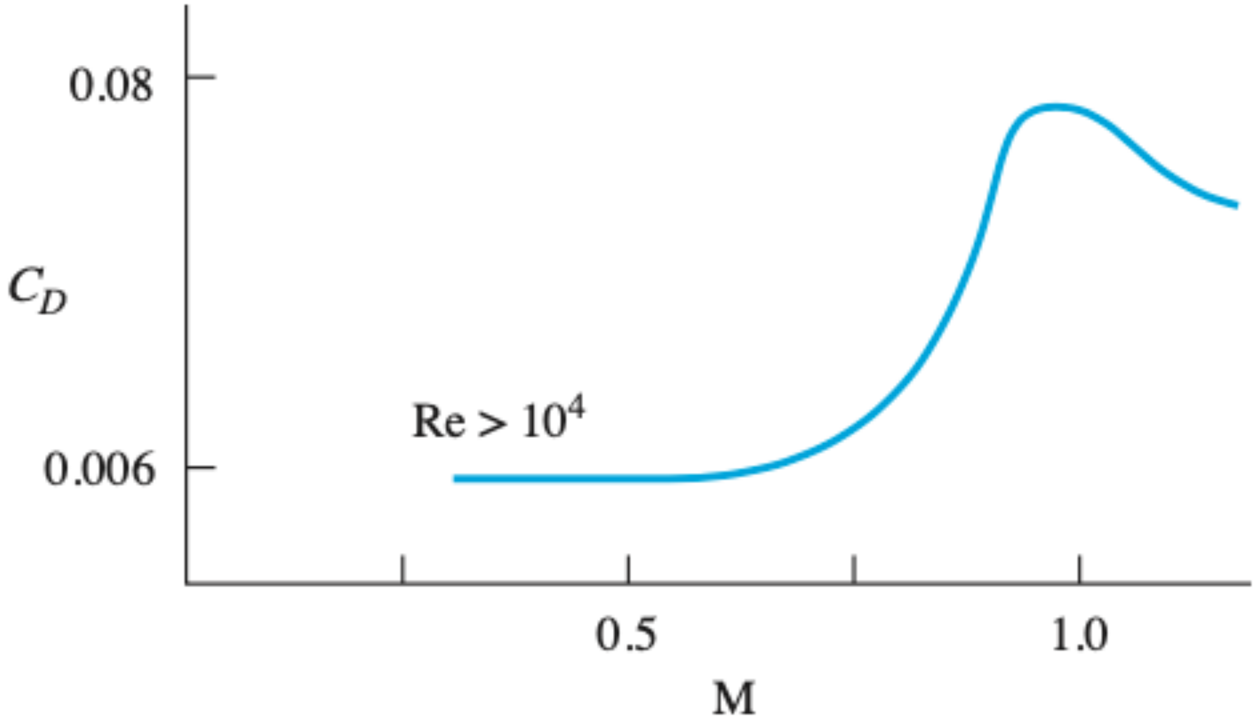

Drag coefficient as a function of Mach number (speed) for a typical unswept airfoil.

It is useful to use swept-back airfoils since it is the component of velocity normal to the leading edge of the airfoil that must be used in calculating the Mach number.

Cruise speeds at $M = 0.8$ with swept-back wings are not uncommon. It should be pointed out, though, that fuel consumption depends on power required, and power is drag force times velocity.

Hence fuel consumption depends on the velocity cubed since the drag force depends on the velocity squared, assuming all other parameters are constant. A lower velocity results in a fuel savings even though the engines must operate longer when traveling a fixed distance.

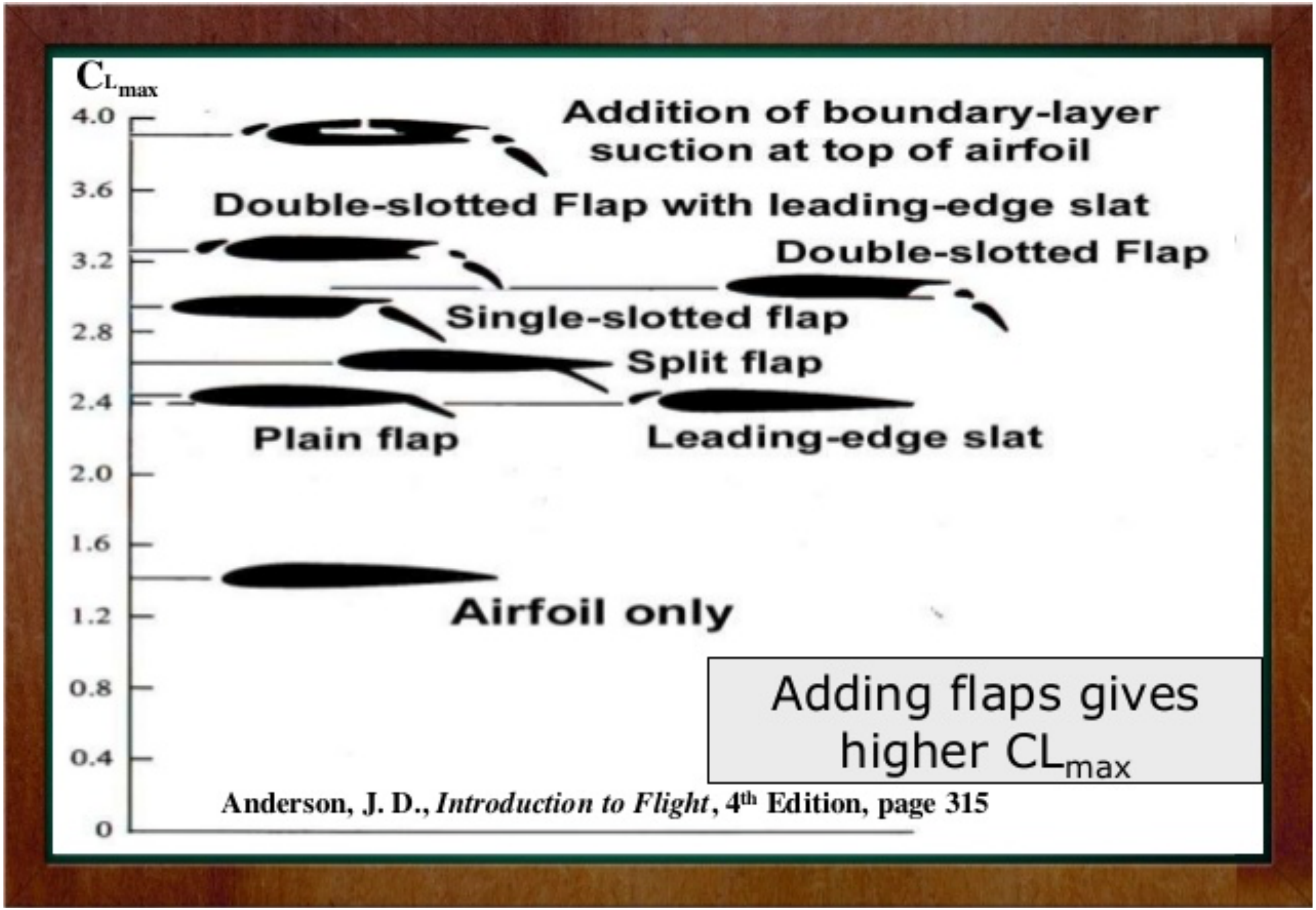

$C_{L_{max}}$
4.0
3.6
3.2
2.8
2.4
2.0
1.6
1.2
0.8
0.4
0
Addition of boundary-layer suction at top of airfoil
Double-slotted Flap with leading-edge slat
Double-slotted Flap
Single-slotted flap
Split flap
Plain flap
Leading-edge slat
Airfoil only
Adding flaps gives higher CL_{max}
Anderson, J. D., *Introduction to Flight*, 4th Edition, page 315

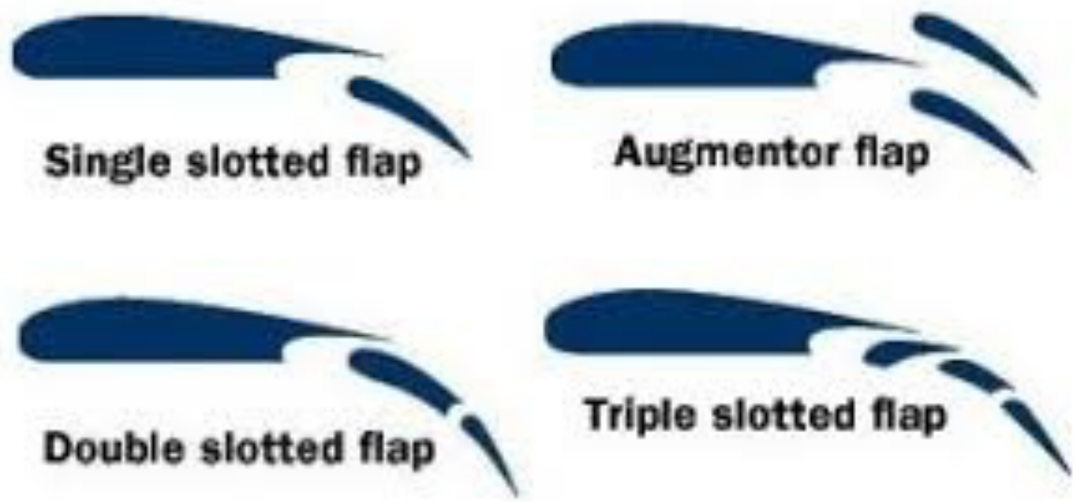
Single slotted flap
Augmentor flap
Double slotted flap
Triple slotted flap

Devices	Increment of max lift	Angle of basic airfoil at max lift	Notes
Basic airfoils 	none	15°	Effect of all high-lift devices depend on shape of basic airfoil.
Plain or camber flap 	50%	12°	Increase camber. Much drag when fully lowered. Nose-down pitching moment.
Split flap 	60%	14°	Increase camber. Even more drag than plain flap. Nose-down pitching moment.

Devices	Increment of max lift	Angle of basic airfoil at max lift	Notes
Zap flap 	90%	13°	Increase camber and wing area. Much drag when fully lowered. Nose-down pitching moment.
Slotted flap 	65%	16°	Control of boundary layer. Increase camber. Stalling delay. Not so much drag.
Double-slotted flap 	70%	18°	Same as single-slotted. Treble slots sometimes used.

Devices	Increment of max lift	Angle of basic airfoil at max lift	Notes
Fowler flap 	90%	15°	Increase camber and wing area. Best flap. Complicated mechanism. Nose-down pitching moment.

Vortex on the airfoil

Fluid particles rotate about the center of a vortex as they travel along in the flow field. There is a high pressure on the bottom and a low pressure on the top side of the airfoil sketched, as shown in the figure below.

This results in a movement of air from the bottom side to the top side around the ends of the air-foil, as shown, resulting in a strong tip vortex.

Distributed vortices are also shed all along the airfoil, and they all collect into two large trailing vortices.

On a clear day, the two trailing vortices may show up as visible white streaks of water vapor behind a high-flying aircraft.

The trailing vortices persist for a considerable distance (perhaps 15 km) behind a large aircraft, and their 90-m/s velocities can cause a small trailing aircraft to flip over.

Also, the trailing vortices induce a downwash, a downward velocity component, that must be accounted for in the design of the aircraft. The tail section is located up high to minimize the effect of this downwash.

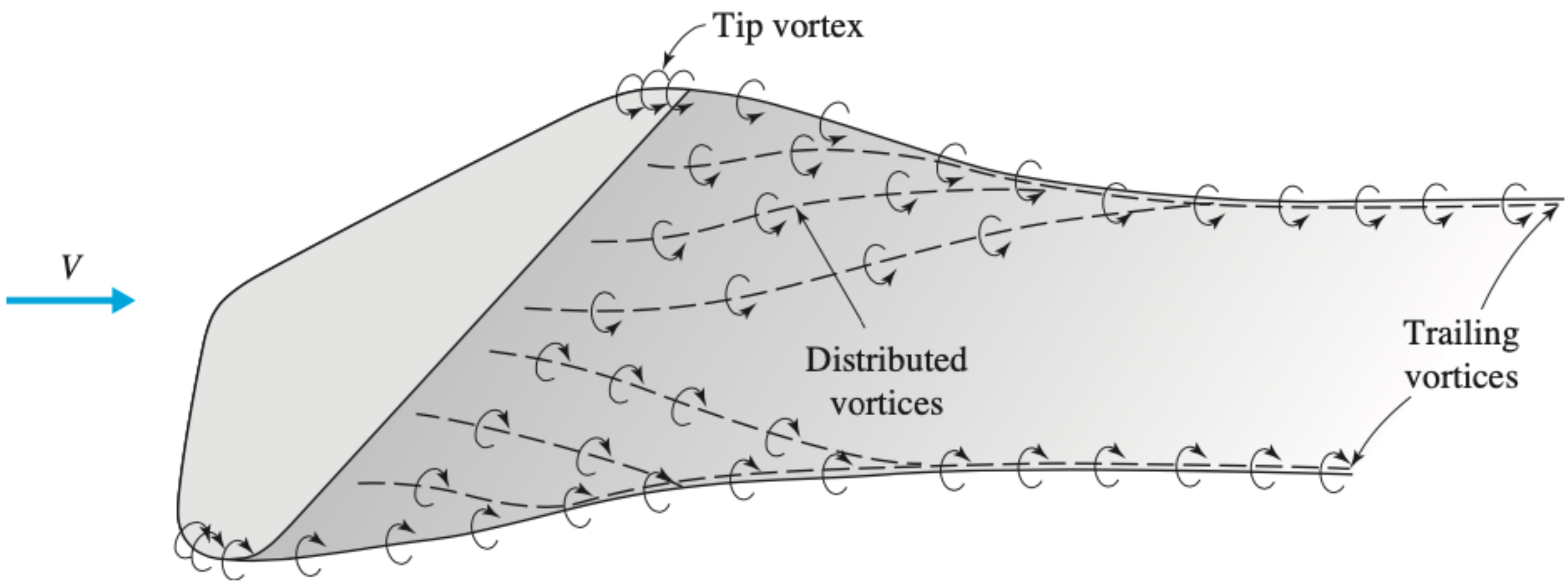

Trailing vortex.

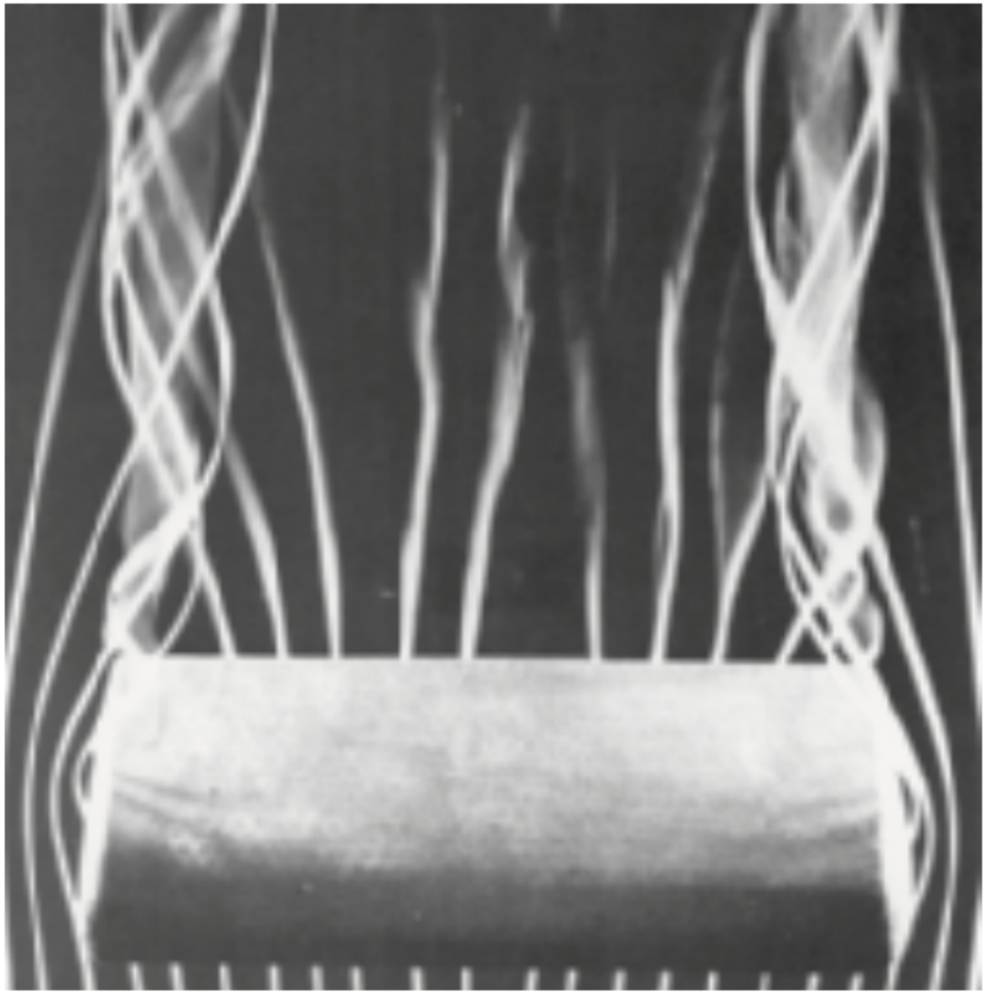

Trailing vortices from a rectangular wing. The flow remains attached over the entire wing surface. The centers of the vortex cores leave the trailing edge at the tips. The model is tested in a smoke tunnel at Reynolds number 100 000. (Photograph by M. R. Head. From Album of Fluid Motion, 1982, The Parabolic Press, Stanford, California.)

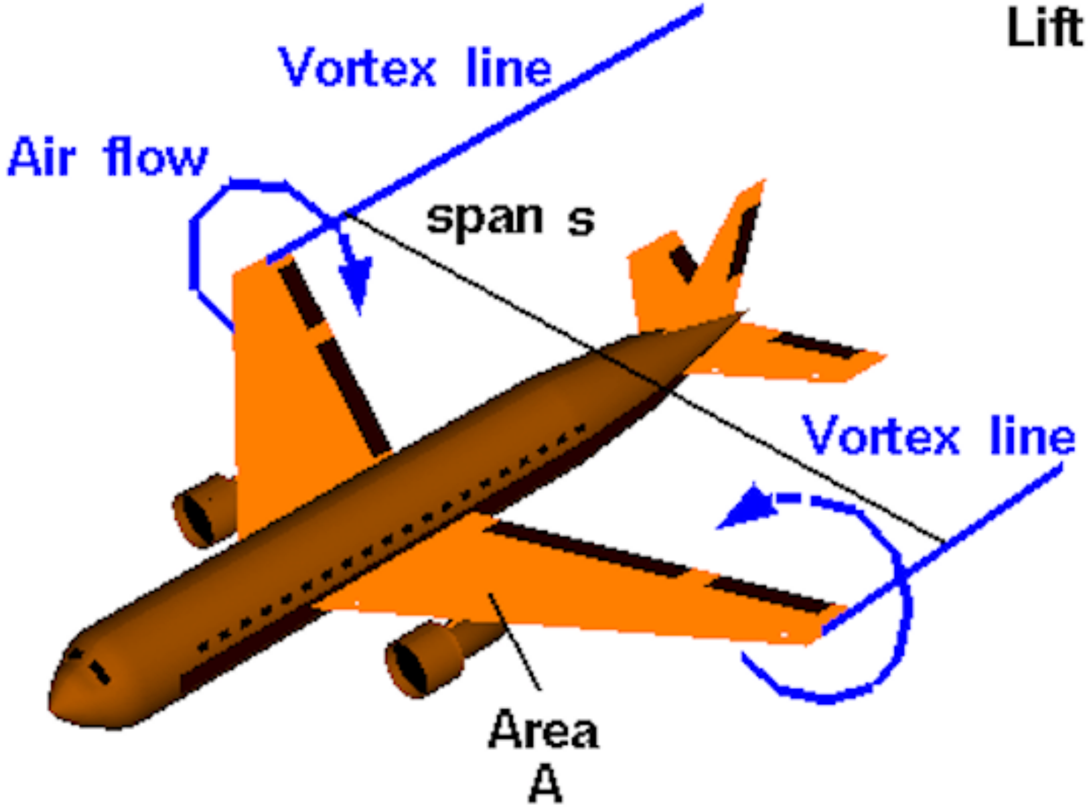

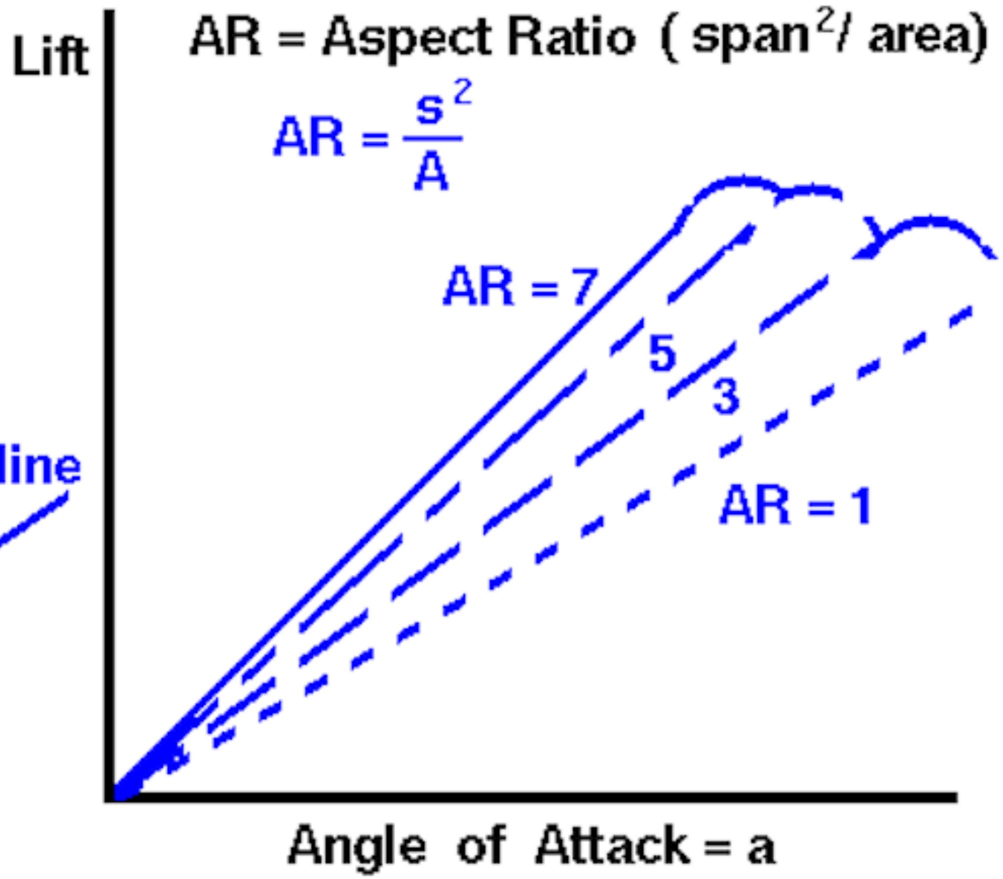

Pressure difference across wing surface causes spillage around wing tips.

Downwash causes a local induced angle of attack which reduces lift.

Lift Coefficient

$$C_l = \frac{C_{lo}}{1 + \frac{C_{lo}}{\pi AR}}$$

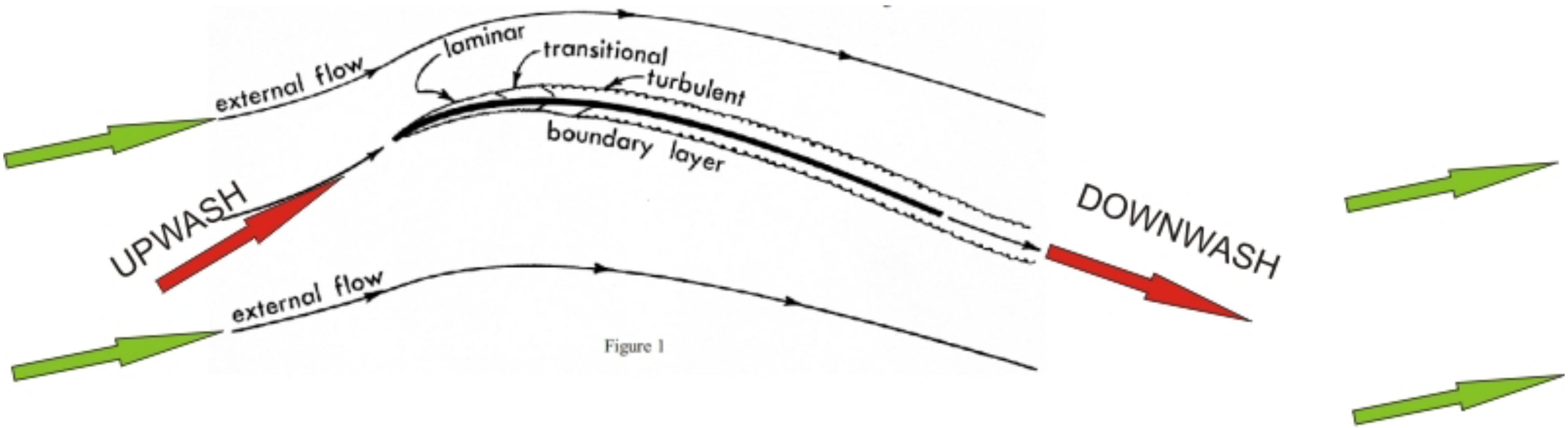

laminar
transitional
turbulent
external flow
boundary layer
UPWASH
DOWNWASH
external flow

Figure 1

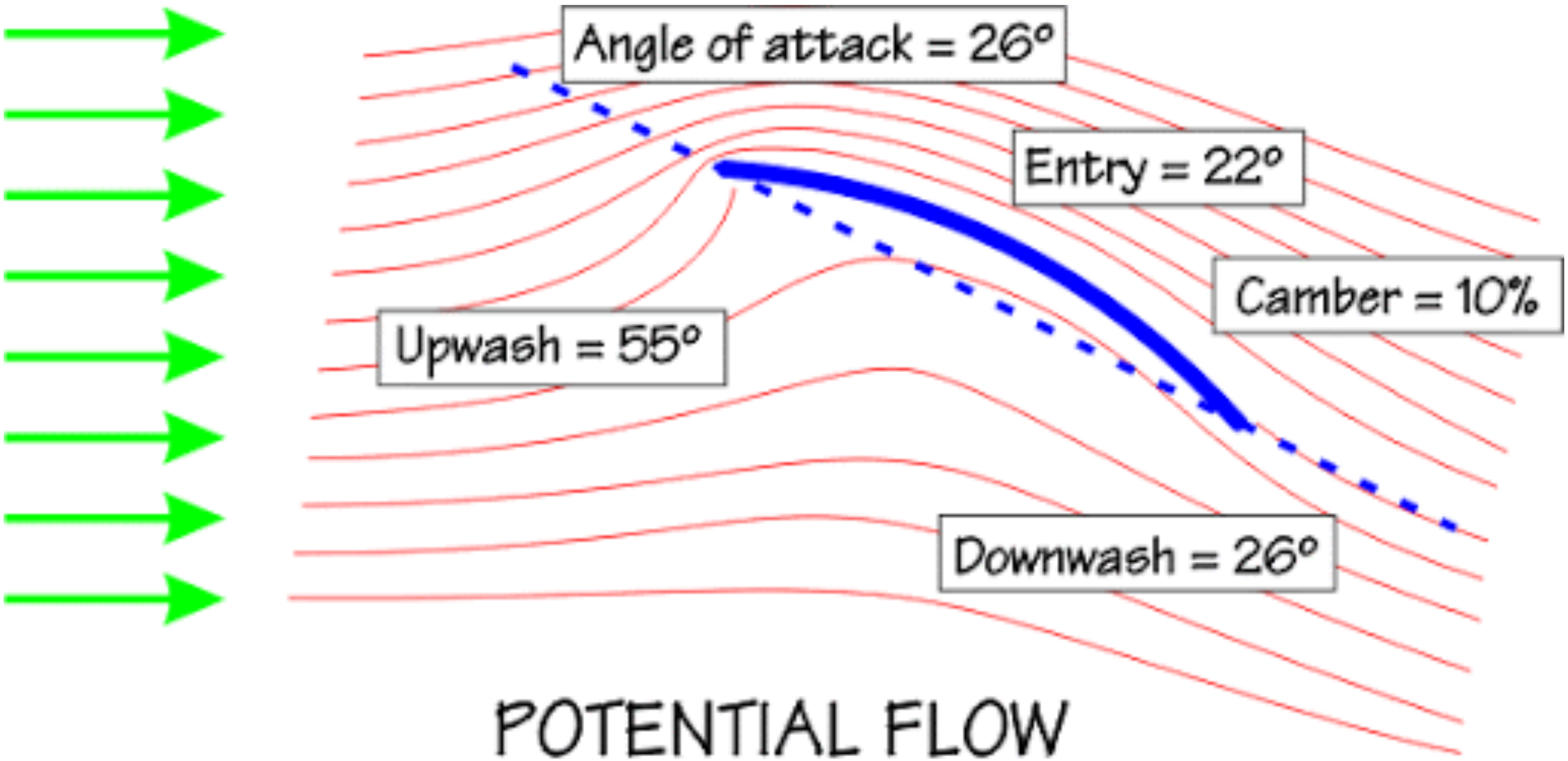

POTENTIAL FLOW

Based on Garrett, Fig. 3.6

Cessna Citationjet Vortices


Photo Copyright © Benjamin Freer
AIRLINERS.NET